PRODUCTION OF COAL-CRUSHER HAMMER HEADS BY BI-METAL CASTING

A THESIS SUBMITTED TO
THE GRADUATE SCHOOL OF NATURAL AND APPLIED SCIENCES
OF
MIDDLE EAST TECHNICAL UNIVERSITY

BY

TURGUT KIRMA

IN PARTIAL FULFILLMENT OF THE REQUIREMENTS
FOR
THE DEGREE OF MASTER OF SCIENCE
IN
METALLURGICAL AND MATERIALS ENGINEERING

SEPTEMBER 2008

Approval of the thesis:

PRODUCTION OF COAL-CRUSHER HAMMER HEADS BY BI-METAL CASTING

submitted by **TURGUT KIRMA** in partial fulfillment of the requirements for the degree of **Master of Science in Metallurgical and Materials Engineering Department, Middle East Technical University** by,

Prof. Dr. Canan Özgen _____
Dean, Graduate School of **Natural and Applied Sciences**

Prof. Dr. Tayfur Öztürk _____
Head of Department, **Metallurgical and Materials Engineering**

Prof. Dr. Ekrem Selçuk _____
Supervisor, **Metallurgical and Materials Engineering Dept., METU**

Prof. Dr. Ali Kalkanlı _____
Co-Advisor, **Metallurgical and Materials Engineering Dept., METU**

Examining Committee Members:

Prof. Dr. Gülhan Özbayoğlu
Mining Engineering Dept., METU _____

Prof. Dr. Tayfur Öztürk _____
Metallurgical and Materials Engineering Dept., METU

Prof. Dr. Ekrem Selçuk _____
Metallurgical and Materials Engineering Dept., METU

Prof. Dr. Ali Kalkanlı _____
Mechanical Engineering Dept., METU

Prof. Dr. Yavuz Topkaya _____
Metallurgical and Materials Engineering Dept., METU

Date : 03.09.2008

I hereby declare that all information in this document has been obtained and presented accordance with the academic rules and ethical conduct. I also declare that, as required by these rules and conduct, I have fully cited and referenced all material and results that are not original to this work.

Name, Last name : Turgut Kırma

Signature :

ABSTRACT

PRODUCTION OF COAL-CRUSHING HAMMER HEADS BY BI-METAL CASTING

Kırma, Turgut

M.Sc., Department of Metallurgical and Materials Engineering

Supervisor : Prof. Dr. Ekrem Selçuk

Co-Advisor : Prof. Dr. Ali Kalkanlı

September 2008, 96 pages

In this study, by considering different mechanical properties such as wear resistance and toughness of two different metal alloys in design and production stages, bi-metal casting technique was used for producing composite material which will be a solution for the cracking and wear problem in coal crushing hammer heads. The failure analysis of the classical hammer heads which are made from Hadfield steels (austenitic steel) showed that there are crack formations through austenitic grains and also the phase transformation from austenite to martensite is not completed until the material consumed its life.

Thermal analysis is the basic technique in this study to determine the solidification conditions. By using thermocouples with a suitable set-up, the cooling curves of the materials which were used in bi-metal casting had been taken and analysed. By using these cooling curve data with a written software program which is based on Newton Thermal Analysis, the solid fraction values by time and by temperate were obtained. According to these values, the interface was investigated by changing experimental conditions and solid fractions. At the last part of the study, a new approach was tried in white cast iron production.

Keywords : Toughness, Wear Resistance, Bi-Metal Casting, Hadfield Steels, Thermal Analysis

ÖZ

KÖMÜR KIRICI ÇEKİÇ BAŞLARININ
Bİ-METAL DÖKÜM YÖNTEMİ İLE ÜRETİLMESİ

Kırma, Turgut
Yüksek Lisans, Metalurji ve Malzeme Mühendisliği
Tez Yöneticisi : Prof. Dr. Ekrem Selçuk
Ortak Tez Yöneticisi : Prof. Dr. Ali Kalkanlı

Eylül 2008, 96 sayfa

Bu çalışmada, iki farklı metal alaşımının dizayn ve üretim sürecinde yüksek aşınma direnci ve tokluk gibi farklı mekanik özellikleri göz önünde bulundurularak, kömür kırıcı çekiç başlarının maruz kaldığı çatlama ve aşınma problemine bir çözüm yaratmak amacı ile bi-metal döküm tekniği kullanılarak kompozit malzeme üretimi incelenmiştir. Hadfield çeliklerinden (östenitik çelikler) yapılan klasik çekiç başlarının hasar analizi yapıldığında, östenit taneleri boyunca çatlakların oluştuğu ve östenit-martenzit faz dönüşümünün tamamlanamadan malzemenin ömrünün tükendiği tespit edilmiştir.

Termal analiz, bu çalışmada katılaşma durumunu incelemede kullanılan ana tekniktir. Uygun bir deney düzeneği ve sıcaklık ölçer ile bi-metal üretiminde kullanılacak olan malzemelerin soğuma eğrileri elde edilmiş ve incelenmiştir. Elde edilen soğuma eğrileri verileri, Newton Termal Analiz yöntemini esas almış bir programda kullanılarak, zamana ve sıcaklığa bağlı katılaşma yüzdeleri elde edilmiştir. Bu değerlere göre, farklı döküm koşullarında ve katılaşma yüzdelerinde çalışılarak, ara yüzey incelenmiştir. Çalışmanın son kısmında, beyaz dökme demir üretiminde yeni bir yaklaşım denenmiştir.

Anahtar Kelimeler : Tokluk, Aşınma Direnci, Bi-Metal Döküm, Hadfield Çelikleri, Termal Analiz

To my Grandmother and Bülent Bolayır ;

ACKNOWLEDGEMENTS

I would like to express my sincere gratitude to my supervisor Prof. Dr. Ekrem Selçuk for his guidance, support and encouragement throughout the study.

I am also grateful to Prof. Dr. Ali Kalkanlı for his insightful comments and helpful advices which encourages me to work harder.

I must also thank to my roommate Arda Çetin for his support in the completion of the thesis and also sharing his valuable knowledge and experiences with me.

I would also like to thank to Salih Türe for his effort during experiments.

I would like to express my sincere thanks to Gökhan Türkyılmaz, Seda Sayılgan, Özgür Keleş, Barış Akgün, Metehan Erdoğan, Emre Ergül, Pelin Maradit, Deniz Keçik, Çağla Özgit, Ebru Saraloğlu, Evren and Elvan Tan and other members of the faculty.

Finally, I want to express my great thanks to my mother and father, Zennure and Ziya Kırma, for their endless love, invaluable trust, support and guidance throughout my life. And also I want to thank to Aslı Erdoğdu and Nevin Genceldi for their moral support and motivation.

TABLE OF CONTENTS

LIST OF TABLES

TABLES

LIST OF FIGURES

FIGURES

CHAPTER 1

INTRODUCTION

For almost a century, the process of size reduction was studied in terms of the energy consumed during the operation of a grinding mill. This was a logical starting point because size reduction is responsible for a large proportion of the costs of ore treatment and the energy consumed is the major cost in size reduction. In coal-fired power generation stations the coal has normally to be crushed and milled before use.

The crushing and milling of the coal was done in a certain case by means of pulverizers whose operating costs were high because of the rapid wear of certain components (which can generally be characterized as wear elements) causing frequent breakdowns and replacements [1]. Wear and crack formation have a great influence on the mill performance and maximization of the equipment's lives is important to the operators and manufacturers.

The crusher hammers are installed at the rotor and rotate at high speed [1]. These hammers are subject to complex stresses following impact and thrust motions, abrasion and in the case of clinker mills frequent high temperatures. Under these conditions the plant operator expects high wear-resistance and toughness as well as 100 % operational safety. The limits of wear resistance using mono-metallic components have been reached. Obtaining high toughness with high wear resistance is a problem for one cast components. Wear on plant components represents a considerable cost factor for the operators of excavating and processing machines. One possible way of improving wear resistance with increasing toughness lies in making components of composite castings [2].

It is advantageous if different materials which self-combine, and therefore can not be detached from one another, are combined in one cast component [2]. This means that one component can contain specific combinations of properties, such as impact resistance and wear resistance and these materials are called bi-materials.

The purpose of this study is try to find the true way to produce the bi-metal which has the highest strength on the interface by the controlling of the thermal conditions during the casting process and to generalize this solution to be applicable for the other applications.

CHAPTER 2

THEORY AND LITERATURE SURVEY

2.1 Coal for Electric Power Generation

Modern life is unimaginable without electricity. It lights houses, buildings, streets, provides domestic and industrial heat, and powers most equipment used in homes, offices and machinery in factories. Improving acces to electricity worldwide is a key factor in alleviating poverty. It is staggering to think that 1.6 billion people worldwide, or 27 % of the world's population, do not have access to electricity [1].

Steam coal, also known as thermal coal, is used in power stations to generate electricity. The earliest conventional coal-fired power stations used lump coal which was burnt on a grate in boilers to raise steam. Nowadays, "the coal is first milled to a fine powder, which increases the surface area and allows it to burn more quickly". In these pulverised coal combustion (PCC) systems, the powdered coal is blown into the combustion chamber of a boiler where it is burnt at high temperature. The hot gases and heat energy produced converts water – in tubes lining the boiler – into steam.

The high pressure steam is passed into a turbine containing thousands of propeller – like blades. The steam pushes these blades causing the turbine shaft to rotate at high speed. A generator is mounted at one end of the turbine shaft and consists of carefully wound wire coils. Electricity is generated when these are rapidly rotated in a strong magnetic field. After passing through the turbine, the steam is condensed and returned to the boiler to be heated once again. (Figure 2.1)

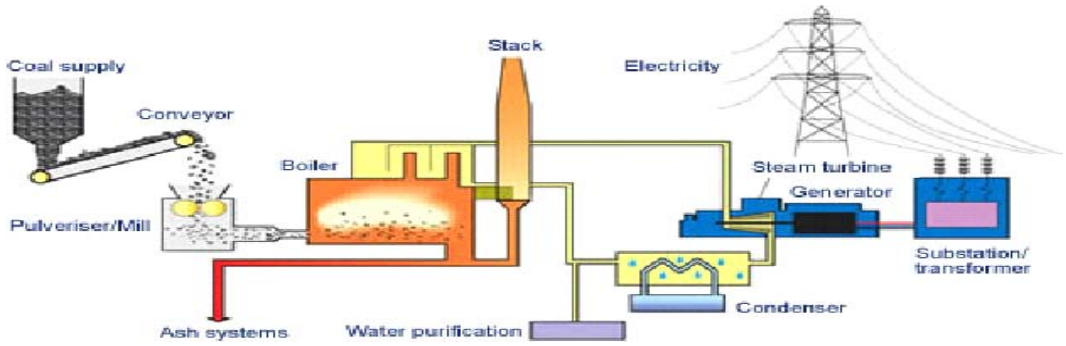

Figure 2.1 Thermal Power Plant [1].

Types of coal are dependent on their contents. Especially carbon contents of them identify their qualities. As shown in Figure 2.2, for power generation systems, lignite is the most useful type of coal which has low carbon content and high silica content which cause abrasive wear.

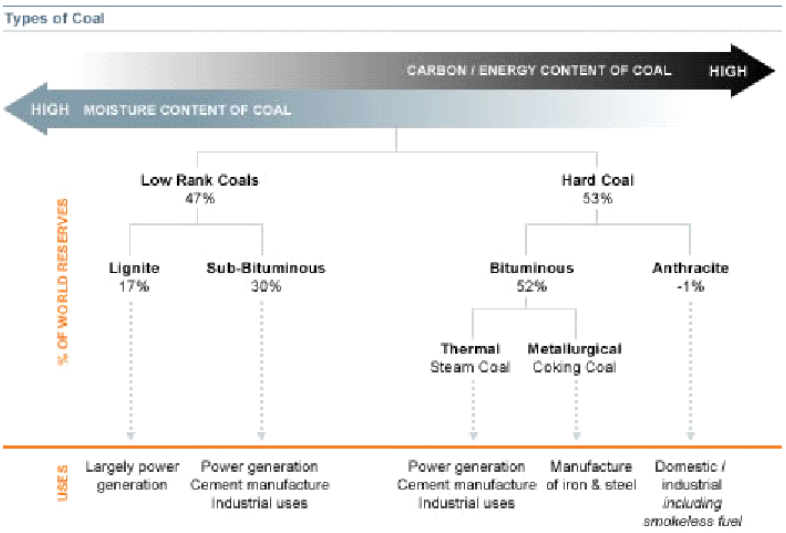

Figure 2.2 Types of Coal [1].

2.2 Size Reduction

Size reduction is responsible for a large proportion of the costs of ore treatment and the energy consumed is the major cost in size reduction. This basis of investigation was influenced more by the economics of the operation than by any other factor. While metallurgists are still interested in reducing costs, they have now approached the problem in a different way, firstly by studying the process of size reduction itself, and secondly by obtaining mathematical relationships linking the operating variables [3].

The purposes of reducing the size of solid particles;

1) To liberate valuable minerals from waste prior to concentration, such as in treatment of metalliferrous ores by flotation.
2) To increase the surface area available for chemical reaction, such as in the reaction of limestone with silica and other minerals in a rotary kiln.
3) To produce mineral particles or dimension stone of required size and shape.

2.2.1 Crushing Theory

The forces used to produce fracture of a perfect crystal are two main types. The structure is bound together by its inter-atomic forces of attraction. If tension is applied the crystal stretches elastically until it reaches its yield point, and recovers if the stress is removed before this point is reached. Once the elastic limit is exceeded a flaw is produced, usually in the form of a minute crack, which becomes a focus for incipient fracture. In his classic paper Griffiths noted that the stress which the crystal can thenceforward withstand is inversely proportional to the square root of the length of the crack. This means that it will now fracture at a much diminished stress loading. During the stressing which created the imperfection, work was done to overcome the mutual bonding of the inter-atomic forces. This work was stored as elastic energy, and was released as the atoms returned to their normal positions.

Since a crack existed, the atoms in its vicinity were able to shed elastic energy while the crystal was being stressed. If this released energy was sufficient to overcome the weakened inter-atomic bonds at the tips of the crack, it grew rapidly (at a speed of about 15,000 ft/sec.) [3].

2.2.2 Grinding

Grinding is the last stage in the comminution process. The ore particles are reduced in size by a combination of impact and abrasion. The grinding process is the largest energy consumer in the mineral industry.

Figures 2.3 and 2.4 shows the Beater Wheel Mill type grinders which are widely used as a coal grinder in thermal power plants in Turkey and also in the other countries of the world.

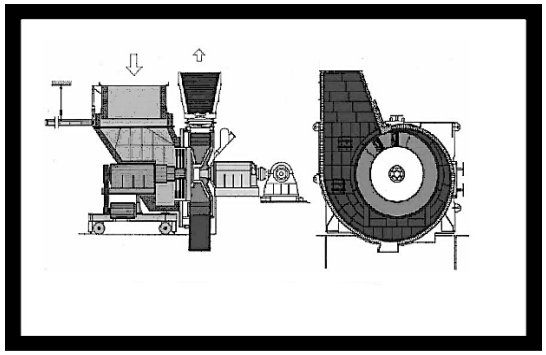

Figure 2.3 Beater Wheel Mill.

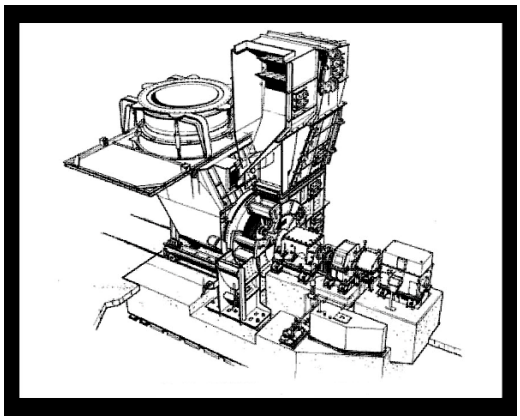

Figure 2.4 Beater Wheel Mill With Prebeater.

2.2.3 Comminution

Crushing, grinding and other words or phrases associated with the size reduction of ore and other rock are all comprehended in the word “comminution”. This is “the whole operation of reducing the crude ore to the fineness necessary for mechanical separation, or for metallurgical treatment”. It is usual to make an arbitrary division of comminution into convenient stages, as shown in Figure 2.5. Primary crushing brings run-of-mine ore down to a maximum size of the order 4” to 6” in average diameter; secondary crushing receives feed at 6” and reduces it below 0.75” [3].

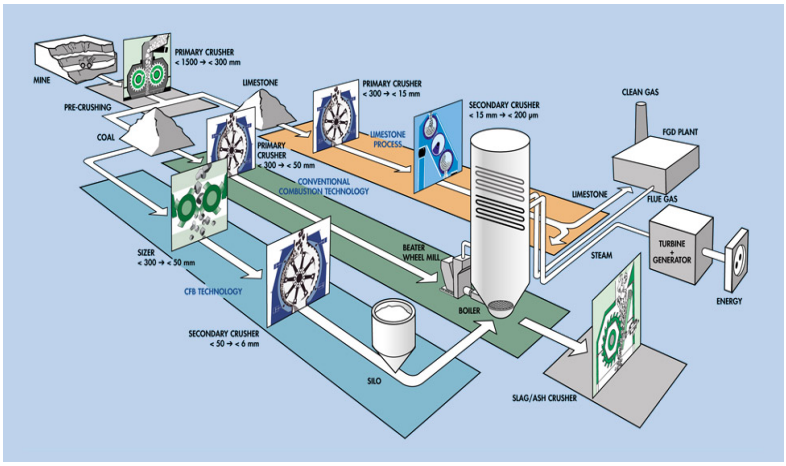

Figure 2.5 Comminution Processes of Coal [5].

Three theories of comminution which have long existed and which have been used with a varying degree of success are the Rittinger, Kick and Bond theories. [5].

The Rittinger theory is the older and more widely accepted. More than 100 years ago Rittinger stated his conclusion that the useful work accomplished in crushing and grinding is directly proportional to the new surface area produced, and to the reciprocals of the product particle diameters.

The Rittinger theory has been amplified and enlarged by Gaudin to include the concept of surface energy. He showed that the efficiency of a comminution operation is the ratio of the surface energy produced to the kinetic energy expended.

The Kick theory which has been in existence for more than 80 years is based primarily upon the stress-strain diagram of cubes under compression. It states that the work required is proportional to the reduction in volume of the particles concerned [5].

The Bond theory claims that crack tip length of the material is inversely proportional with the square root of the product particle diameter.

As shown in Figure 2.6, there are different machine parts which are used in coal crushers and grinders, such as hammer heads and impact bars. According to their chemical compositions, it is seen that these machine parts are made from Hadfield steels, in other words high manganese steels.

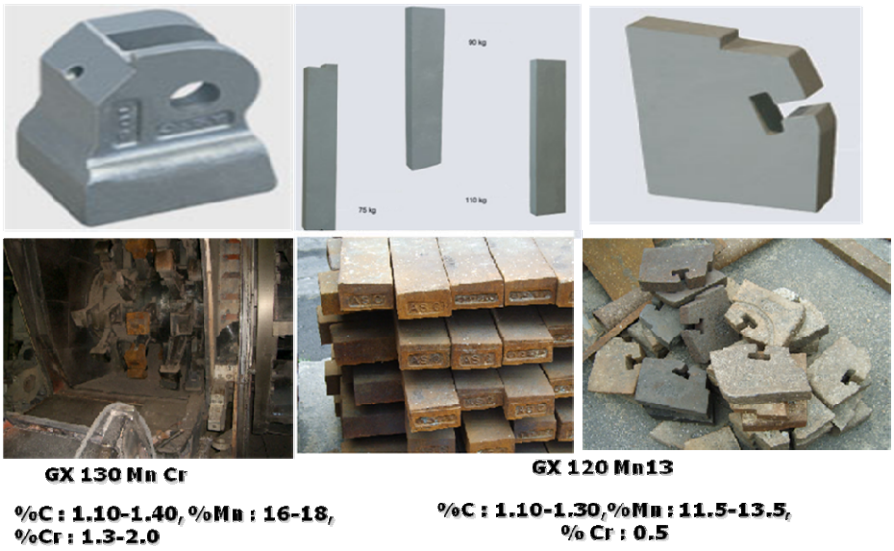

Figure 2.6 Communition Machine Parts and Their Materials.

2.3 Crusher Hammer Design

Impact breakers, impact crushers, and hammer mills accomplish material breaking and reduction primarily through impact action of the material with fixed or free-swinging hammers revolving about a central rotor. The material to be crushed enters through an opening at the top or top side known as the “feed opening” or “hopper opening” and falls into the path of rotation (hammer circle) of the hammers. Initial breakage is accomplished in midair by collision of the dropping feed material with high-speed hammers. The second stage of breakage occurs when the pieces hit plates or breaker bars which line the crusher boxlike frame [4].

The term hammer is used in reference to the piece which strikes the material, whether it is fixed on the rotor or free-swinging. Hammers may be mounted in two, three, four, or six rows. The number of hammer rows varies by manufacturer [4].

Hammer design plays a significant role in crusher efficiency, because in most types of crushers, the hammers do most of the work. Early hammer designs were only concerned with mass and general shape of the hammer. (Figure 2.7).

The crusher hammers are installed on the rotor spins and rotate at high speed. These hammers are subject to complex stresses following impact and thrust motions and abrasion.

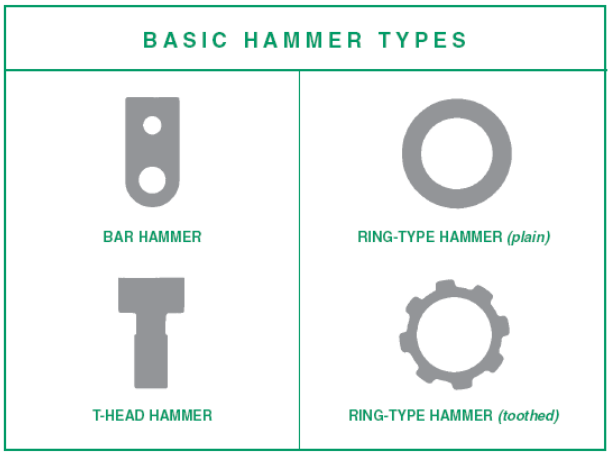

Figure 2.7 Basic Hammer Heads [4].

2.4 Wear

Wear, defined as unwanted material removal, is damage to a solid surface as a result of relative motion between it and another surface or substance. The damage usually results in the progressive loss of material. The scientific measure used for wear is volume loss. However, in engineering concern with wear is usually associated with dimensional or appearance changes that eventually affect performance and not with volume loss. As a result other measures are often used in practice, such as depth of the wear scar on a mechanical component or the degree of haze with optical components.

For any material, wear can occur by a variety of mechanisms, depending on the properties of the material and the situation in which it is being used, as shown in Figure 2.8. Generally, more than a single mechanism occur at the same time.

However, there is always a primary mechanism that determines the material removal rate. Whenever there is a possibility of abrasive wear, it is the most important problem to be solved. The wear rate of abrasive wear is at least one to two orders of magnitude larger than those of other mechanisms [6].

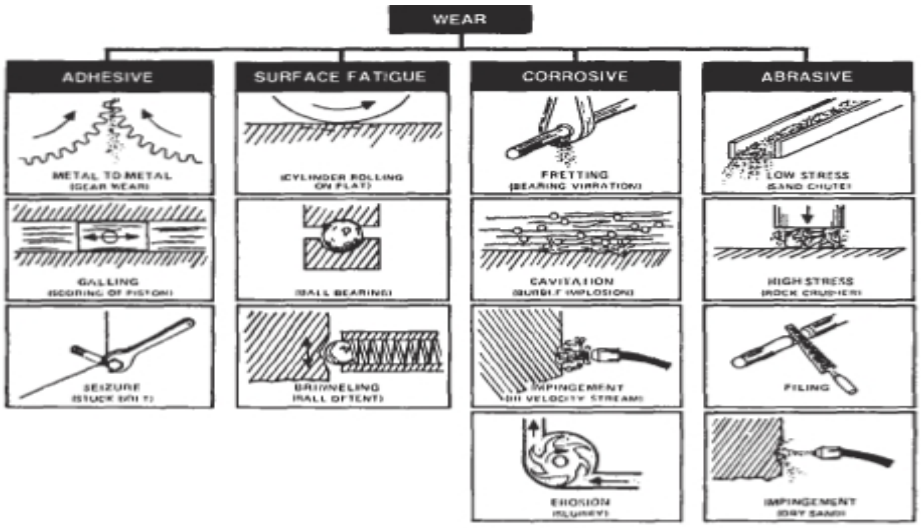

Figure 2.8 Wear Mechanisms [6].

If the harder surface is rough or if hard abrasive particles are present, abrasive wear may be the dominant mechanism. In the theory of abrasive wear, it is assumed that each abrading element is so hard (rather than rounded) so as to indent the opposing surface [6].

Wear resistance is, of course, a compromise with all the other required properties of the material (strength, corrosion resistance, matching thermal expansions, dimensional stability, weldability, etc.) and the significance or competing failure modes (fatigue, corrosion, fracture, creep, etc.) [6].

Wear resistance is not an intrinsic material property like hardness or elastic modulus. Both wear and wear resistance are system properties or responses.
Collection of all the mechanical, chemical, and environmental elements that can affect wear behaviour is referred to as the tribosystem. Typical factors that can

affect wear behaviour are the properties of the materials, the nature of the relative motion, the nature of the loading, the shape of the surface, the surface roughness, the ambient temperature, and the composition of the environment in which the wear occurs. Tribosystem design parameters are those parameters that affect wear and that the designer can specify and alter. Designing for the control of wear involves selecting values for tribosystem design parameters in order to obtain acceptable wear behaviour or life. The process for doing this is called wear design.

2.5 Hadfield Steels

The original austenitic manganese steel containing about 1.2 % C and 12 % Mn, was invented by Sir Robert Hadfield in 1882. It was unique in that it combined high toughness and ductility with high work-hardening capacity and usually good resistance to wear [7]. Austenitic Hadfield steel containing about 1.2 % C and 12 % Mn is known for a high resistance to impact wear caused by rapid cold work hardening, for which different mechanisms were proposed. An early explanation pointed to strain-induced $\gamma \rightarrow \varepsilon$ martensitic transformation [8].

Hadfield austenitic manganese steel is still used extensively, with minor modifications in compositions and heat treatment. As shown in Table 2.1, this steel allows composition ranges from 1.0 to 1.4 % C and from 10 to 14 % Mn. However, commercial alloys with manganese contents greater than 12 to 13 % are seldom used because of cost. Moreover, work hardening in a 1.15 % C alloy reaches a maximum at 13 % Mn. Hadfield steel is usually austenized to dissolve carbides and to produce homogeneous austenite, which is preserved by water quenching from above 1000 °C . So it is a stable, single phase, austenitic alloy which is annealed and quenched before use to retain all the carbon in supersaturated solid solution.

Typical properties are 0.2 % offset yield strength 379 MPa, ultimate tensile strength 965 MPa, elongation in 50 mm 50 %, reduction of area 40 %, as-quenched hardness 190 HB, hardness, at fracture, 500 HB [7,9].

To modify Hadfield steels' properties, especially wear resistance, alloying elements are used. So the selection of right alloying element and its quantity and also required heat treatment is critical. Results of mechanical tests should be supported by metallographic findings to make the phenomena more clear.

Hadfield steels are used in a variety of applications, for example, railroads, grinding mill liners, crusher jaws and cones, impact hammers and bullet-proof helmets. The mechanical properties of Hadfield steel vary with both carbon and manganese contents. The tensile strength and ductility reach a maximum limit at about 1.2 % C content and then decrease steadily as the carbon content is increased [10].

Austenitic manganese steel resists metal to metal wear; therefore it may be used in sprockets, pinions, gears, wheels, conveyor chain and various wearing plates, shoes or other contact members.

To improve the wear resistance of austenitic manganese steels without, at the same time, seriously injuring their toughness, a logical approach appeared to lie in the production of the properly dispersed hard carbides in the austenitic matrix of the steel. Increasing the carbon in the solution in the austenite is also another approach. It has been observed however that in the conventional Hadfield manganese steel, an increase in the carbides, or the carbon in solution, was usually accompanied by the formation of embrittling-type carbide envelopes around grain boundaries or as plates along crystallographic planes. To avoid such embrittlement, the form in which the carbides occurred in the austenite would obviously have to be modified, either by addition of other alloying elements or by special thermal treatments [7].

Hadfield steel is heat treated to a single-phase austenite which is a tough phase. Intergranular embrittlement occurs when grains loose cohesion because intermeditary phases are most notably the presence of hypereutectoid carbide resulting from a slow quench or reheating through the 400 °C – 800 °C range. The degree of embrittlement depends on the degree of grain boundary coverage and the loss of cohesion of the austenite matrix, by the second phases [11].

Table 2.1 Standard Composition Ranges for Austenitic Manganese Steel Castings, ASTM Standard A-128-64.

ASTM A128 Grade	C %	Mn %	Cr %	Mo%	Ni %	Si % (max)	P % (max)
A	**1.05 - 1.35**	**11.0 min**	-	-	-	**1.00**	**0.07**
B-1	**0.9 - 1.05**	**11.5 - 14**	-	-	-	**1.00**	**0.07**
B-2	**1.05 - 1.2**	**11.5 - 14**	-	-	-	**1.00**	**0.07**
B-3	**1.12 - 1.28**	**11.5 - 14**	-	-	-	**1.00**	**0.07**
B-4	**1.2 - 1.35**	**11.5 - 14**	-	-	-	**1.00**	**0.07**
C	**1.05 - 1.35**	**11.5 - 14**	**1.5 – 2.5**	-	-	**1.00**	**0.07**

2.6 Cast Iron

Cast iron is essentially an iron-carbon alloy containing other important elements such as silicon, manganese, sulphur and phosphorus, which modify the structure and properties of the resulting alloy markedly [12].

As seen in Iron-Carbon phase diagram, Figure 2.9 , cast irons have more than 2 % carbon with a high silicon concentrations and a greater concentration of impurities than steels. The carbon equivalent (CE) of a cast iron helps to distinguish the grey irons which cool into a microstructure containing graphite and the white irons where the carbon is present mainly as cementite [13]. The carbon equivalent is defined as:

$$CE(wt\%) = C + \frac{Si + P}{3} \tag{2.1}$$

A high cooling rate and a low carbon equivalent favours the formation of white cast iron whereas a low cooling rate or a high carbon equivalent promotes grey cast iron.

During solidification, the major proportion of the carbon precipitates in the form of graphite or cementite. When solidification is just complete, the precipitated phase is embedded in a matrix of austenite which has an equilibrium carbon concentration of about 2 wt %. On further cooling, the carbon concentration of the austenite decreases as more cementite or graphite precipitates from solid solution. For conventional cast irons, the austenite then decomposes into pearlite at the eutectoid temperature. However, in grey cast irons, if the cooling rate through the eutectoid temperature is sufficiently slow, then a completely ferritic matrix is obtained with the excess carbon being deposited on the already existing graphite [13].

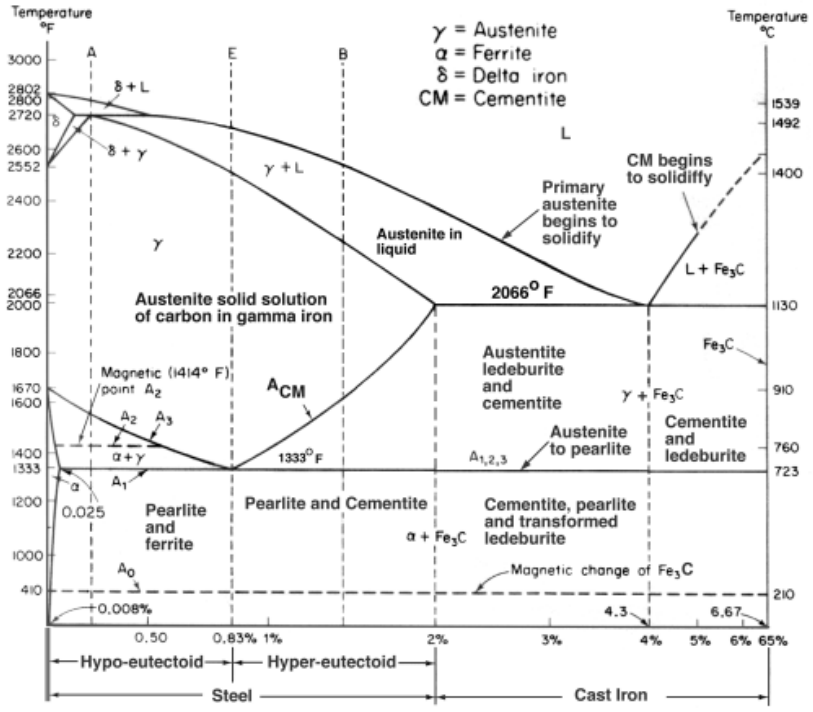

Figure 2.9 Iron – Carbon Phase Diagram.

2.6.1 White Cast Iron

If the iron is sufficiently below the eutectic value, has a very low silicon content, contains appreciable quantities of carbide, stabilising elements, or if the cooling rate is sufficiently rapid, the formation of graphite does not ocur, solidification taking place first by the formation of austenite dendrites, and the interdendritic areas will remain high in carbon and solidify as a eutectic of iron carbide and austenite, known as ledeburite. As the solid casting cools down, at a temperature of 720-750 °C, the austenite, which is γ iron with carbon in solution, transforms to a α iron, in which carbon is substantially insoluble. Carbon is then rejected as iron carbide in the form of lamellae alternative with lamellae of α iron to form a matrix of pearlite. The initially formed iron carbide, however, remains unchanged [12].

The structure of a white iron at room temperature, therefore, consists of primary dendrites of pearlite with interdendritic areas of transformed ledeburite, which is a eutectic structure of iron carbide and pearlite, the pearlite areas having been formed from the original austenite. In some cases, the austenite produced during the final eutectic solidification of iron carbide and austenite is deposited on the already existing austenite dendrites, and the interdentritic area will be predominantly carbide. The final structure will than consist of dendrites of pearlite surrounded by cementite containing very little transformed eutectic pearlite [12].

2.6.2 High Chromium White Cast Iron

High-chromium white cast irons are used extensively in environments where small particle impact causes considerable damage. Very high abrasive wear resistance combined with relatively low production costs make these alloys particularly attractive.

High-chromium white cast irons are used in severe conditions where extreme erosion and abrasion resistance is necessary. These materials are used in grinding, milling and pumping apparatus to process hard materials such as ore, coal, gravel and cement [14-15]. Their exceptional abrasive and erosive wear resistance results

primarily from their high volume fraction of hard carbides, although the toughness of the matrix also contributes to the wear resistance [16].

The typical microstructure of high-chromium white cast irons, shown in Figure 2.10, consist of chromium carbides of high hardness dispersed in a matrix which still contains a sufficient concentration of carbon to allow hardening as a result of transformation of austenite to martensite. This occurs after a quenching treatment. These materials, after tempering, are used in ambient temperature services and also at moderate temperatures (below 500 °C).

The shaping of all these products is carried out by means of casting techniques, applied from the liquid state. These hypoeutectic cast irons start their solidification with the nucleation of austenite dendrites and then continue with the formation of the eutectic constituent $\gamma + M_7C_3$. During cooling, significant quantities of the same carbides precipitate as a result of reduction in carbon solubility [17].

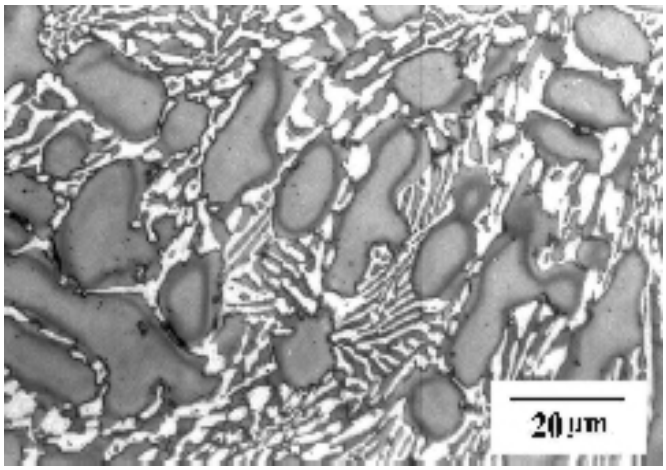

Figure 2.10 Microstructure of High Chromium White Cast Iron [13].

In abrasion-resistant cast irons the Cr content is in the range of 14–28 %; the chromium goes entirely into the carbide phase and serves to enhance the carbide stability, shown in Table 2.2. For lower amounts of Cr in this range, the carbides are generally M_3C. When the amount of Cr is higher, the as-cast structure consists of discontinuous $(CrFe)_7C_3$ carbides and the γ phase which may be completely or partially transformed to martensite during cooling. For the wear resistant materials of concern, it is desirable to have a martensite matrix [15].

Table 2.2 Standard Composition Ranges for Abrasion-Resistant Cast Irons, ASTM Standard A 532/A 532M-93a.

Class	Type	Designation	C %	Mn %	Si %	Ni %	Cr %	Mo %
I	A	Ni-Cr-Hc	2.8-3.6	< 2.0	< 0.8	3.3-5.0	1.4-4.0	<0.3
I	B	Ni-Cr-Lc	2.4-3.0	< 2.0	< 0.8	3.3-5.0	1.4-4.0	<0.3
I	C	Ni-Cr-GB	2.5-3.7	< 2.0	< 0.8	< 4.0	1.0-2.5	<0.3
I	D	Ni-HiCr	2.5-3.6	< 2.0	< 2.0	4.5-7.0	7-11	<0.1
II	A	12 % Cr	2.0-3.3	< 2.0	< 1.5	< 2.5	11-14	<0.1
II	B	15%CrMo	2.0-3.3	< 2.0	< 1.5	< 2.5	14-18	<0.1
II	D	20%CrMo	2.0-3.3	< 2.0	1.0-2.2	< 2.5	18-23	<0.1
III	A	25 % Cr	2.0-3.3	< 2.0	< 1.5	< 2.5	23-30	<0.1

Heat treatment of these products consists of austenitization at a high enough temperature to dissolve most of the carbides that have precipitated in the previous cooling. A high-alloyed austenite with high carbon content is thus obtained. This is partially transformed into martensite by an appropriate quench. However, a significant fraction of retained austenite remains after the hardening treatment and must be completely eliminated by applying two or more tempering heat treatments.

In the course of these tempering treatments, substantial structural hardening takes place (secondary hardening), resulting from a uniform precipitation of very fine carbides, along with the transformation of retained austenite to martensite. The tempering temperature limits the maximum service temperature allowed for the product. After two or even three tempering treatments, final room temperature hardness of between 600 and 800 HV can be obtained .

2.6.3 Grey Cast Iron

Silicon is as important as carbon element in cast irons, shown in Figure 2.11. Silicon is essential to making of grey cast iron as opposed to white cast iron [18]. It causes the carbon to rapidly come out of solution as graphite, leaving a matrix of relatively pure, soft iron. Weak bonding between planes of graphite lead to a high activation energy for growth in that direction, resulting in thin, round flakes. This structure, shown in Figure 2.12, has several useful properties [19].

Graphite acts as a lubricant, improving wear resistance. The form and distribution in which graphite is deposited depends on numerous factors, such as melting temperature, nucleation, cooling speed, etc. , but the basic forms are flake graphite, aggregate or temper carbon, and nodules or spheroids [12]. The exceptionally high speed of sound in graphite gives cast iron a much higher thermal conductivity. Since ferrite is so different in this respect (having heavier atoms, bonded much less tightly) phonons tend to scatter at the interface between the two materials. In practical terms, this means that cast iron tends to “damp” mechanical vibrations (including sound), which can help machinery to run more smoothly.

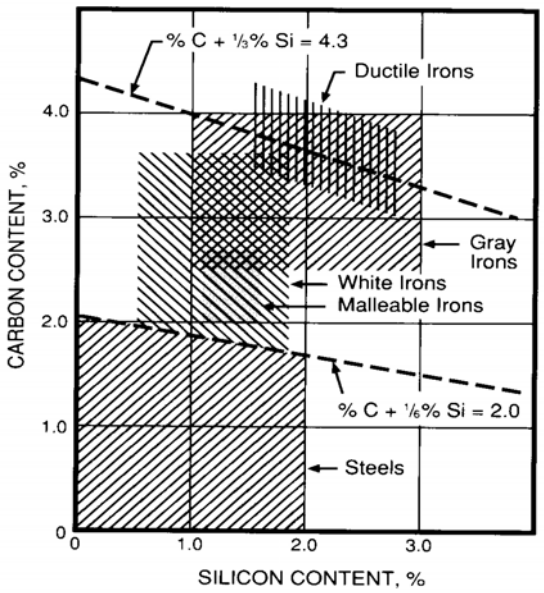

Figure 2.11 Approximate Ranges of Carbon and Silicon for Steel and Various Cast Irons [18].

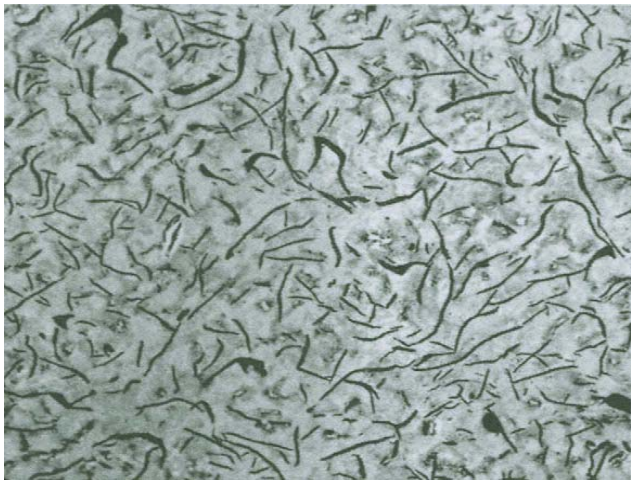

Figure 2.12 Random Flake Graphite, 4 % Picral, 100 X, [19].

2.6.4 Ductile / Nodular Cast Iron

Ductile cast iron, frequently referred to as nodular or spheroidal graphite iron, is a recent member of the family of cast irons. It contains spheroid graphite in the as

cast condition, shown in Figure 2.13, through the addition of nucleating agents such as cerium or magnesium to the liquid iron [12].

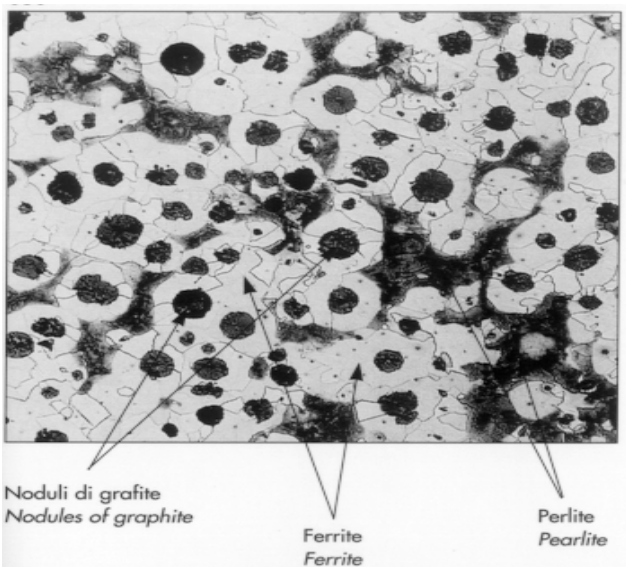

Figure 2.13 Ductile Iron.

In fact ductile cast iron provides a wide spectrum of mechanical properties that can be obtained either by altering certain processing variables or through various heat treatments which present different and better combination of properties for application with special requirements. Elastic behaviours of iron and steel can be seen from Figure 2.14.

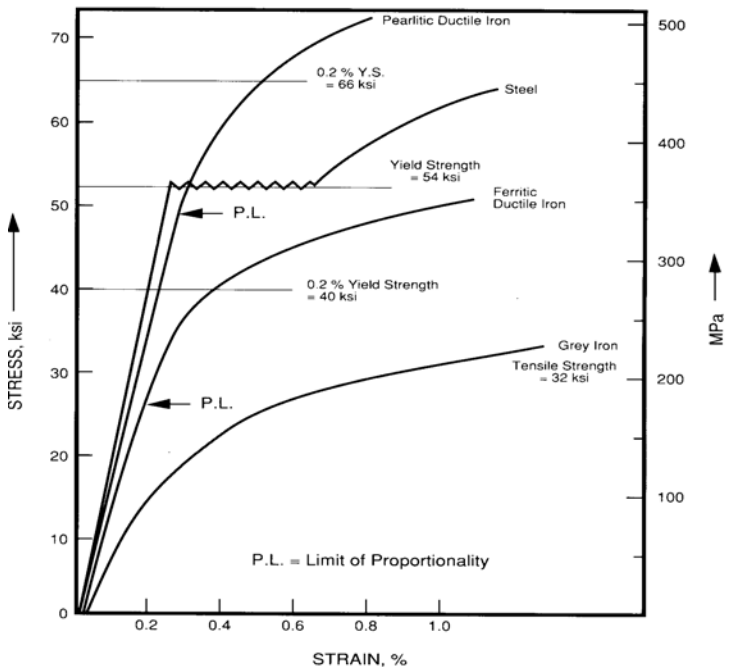

Figure 2.14 Elastic Behaviours of Iron and Steel [18].

2.7 Bimetals

Bi-metal casting technique used for producing composite materials by considering different mechanical properties, corrosive resistance properties and superiorities of two different metal alloys in design and production stages [20]. The secret of the different methods to produce bi-metal castings is that between both alloys used with different characteristic profiles, similar to hardfacing, a compound is formed with little mixing. By means of this combination, however, the wear-resistant casting does not become tough and the tough steel does not become wear-resistant. This combination therefore is only used for such wear parts where different sections are exposed to wear or mechanical stress [21] .

In Figure 2.15, the classic values for abrasion resistance against scratching wear as well as the toughness of such alloys specified below which are normally used for this purpose are shown. Highly abrasion-resistant are those alloys having a hard matrix and, if possible, additional hard carbides in their microstructure. However, such alloys are not tough, as a rule, and therefore subject to breaking.

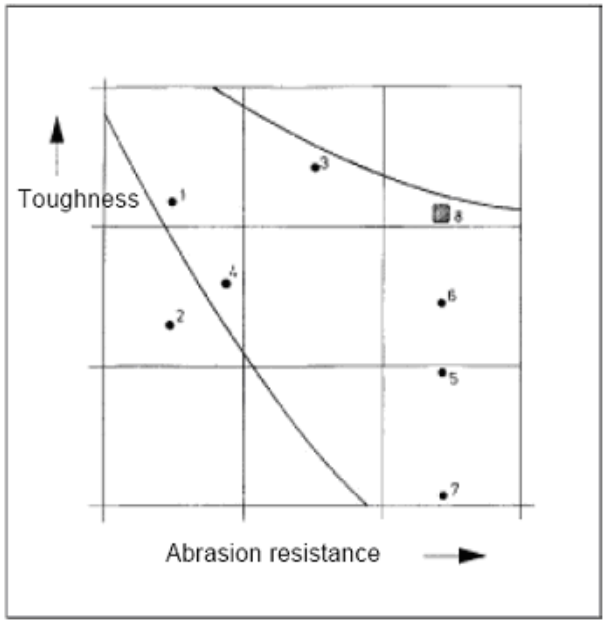

1. GS 45
   Elongation: ≥ 22%
2. GGG 60
   Elongation: ≥ 3%
3. Hard manganese steel casting
   Elongation: ≥ 40%
4. Alloyed, hardened steels with small alloy shares, as a rule smaller than 5 %
   Elongation: ≥ 10%
5. VAUTID W3
   Elongation: < 1%
6. VAUTID W73
   Elongation: < 1%
7. VAUTID hard ceramics
   Elongation: 0%
8. VAUTID bimetal
   Combination of a tough steel casting with wear casting:
   Elongation: ≥20% / < 1%

Figure 2.15 Toughness and Abrasion Resistance of Such Alloys and Bi-metal [20].

There are different applications and methods of bi-metals like hammer heads, impact bars and extruder screws.

As shown in Figure 2.16, bi-metal casting technique is particularly suitable for the production of parts like hammers which need to be tough in the whole area and are exposed to abrasion in the upper part. Here the ratio between hard casting and base body can be adjusted in such a way as it is provided tough by the size of the worn-out wear part when disassembled [22].

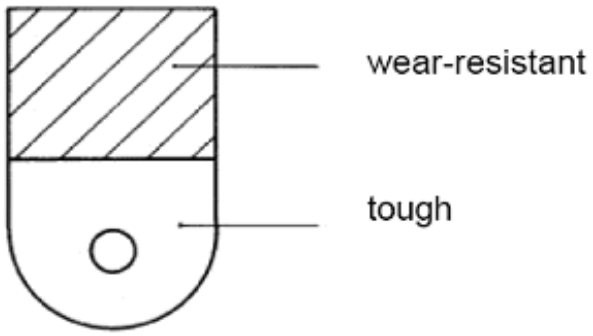

Figure 2.16 Bi-Metal Hammer Head.

As shown in Figure 2.17, this method is suitable for the production of impact bars of very different casting weights where the wear-resistant top edges are made from hard casting. The ratio of wear deposit to tough intermediate body is determined according to the maximum wear volume resulting from the functional size when disassembled.

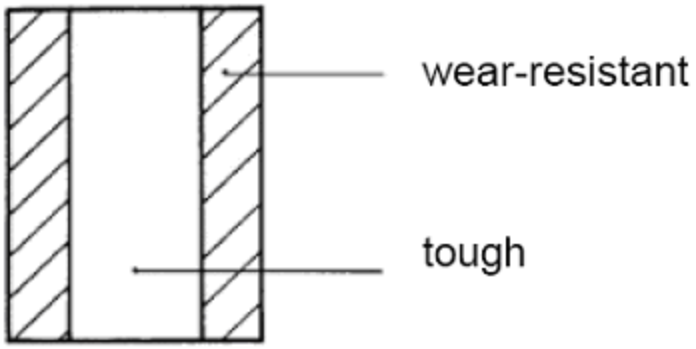

Figure 2.17 Bi-Metal Impact Bar.

As shown in Figure 2.18, according to this method round parts can be produced in the same way as square parts, e.g. bi-metal parts for extruder screws, parts for rolling crushers, segments, etc. [22].

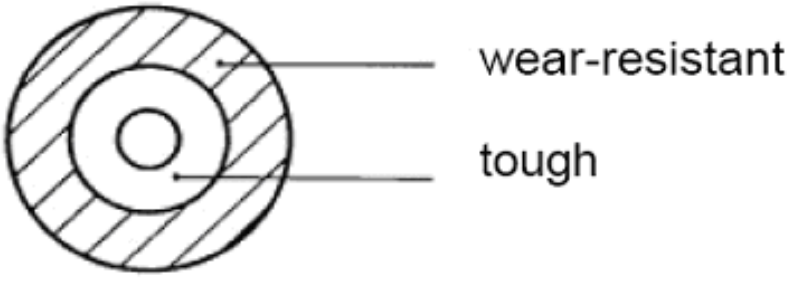

Figure 2.18 Bi-Metal Round Parts.

As can be seen from Figure 2.19, bi-metallic hammer heads' wear rate is lower than monometallics. Thus, bi-metallic parts have longer life time.

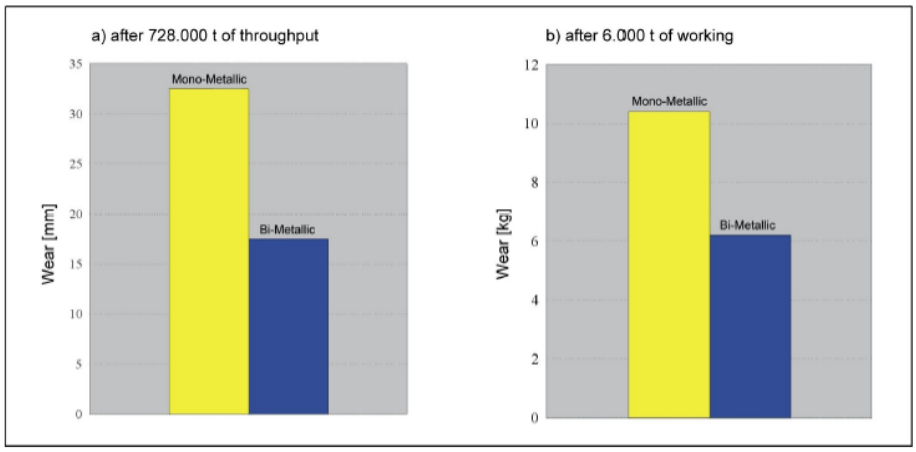

Figure 2.19 Wear of the Bi-Metallic Hammer Head Compared with Mono-Metallics [2].

CHAPTER 3

EXPERIMENTAL PROCEDURE

In this study; the failure analysis of Hadfield steel machine parts which are used in coal crushers and grinders was made and evaluated. After evaluation, bi-metal applications were found as a solution for the wear problem which is seen in Hadfield steel. The production of bi-metals is the main point of this study. At the first part of experiments, the unalloyed cast irons were used. At the second part of experiments, the alloyed cast irons were studied. Finally, the results were evaluated and some improvements had been made. Thermal analysis was used as a basic technique while producing bi-metal coal crusher hammer head and impact bar instead of Hadfield steels.

3.1 Material Used

This research aims at producing bi-metal products with using a wear resistant material and tough material. For the first part of the bi-metal production experiments; unalloyed white cast iron was choosen as a wear resistant material and grey iron was choosen as a tough material. At the second part of the bi-metal production experiments, high chromium white cast iron was used as a wear resistant material whereas ductile iron was used as a tough material. In addition to bi-metal experiments, an improvement study was made in white cast iron production with Mischmetal addition as an alloying element.

Table 3.1 Chemical Composition of Unalloyed White Cast Iron and Grey Cast Iron.

Unalloyed Materials	C %	Si %	P %	S %	Carbon Equivalent
White Cast Iron	3.2	1.18	0.006	0.003	3.6
Grey Cast Iron	3.5	2.4	0.01	0.003	4.3

Table 3.2 Chemical Composition of Alloyed White Cast Iron, Grey Cast Iron and Ductile Iron.

Alloyed Materials	C %	Si %	P %	S %	Mg %
5.2 % Cr White Cast Iron	3.78	0.78	0.053	0.015	-
10.5 % Cr White Cast Iron	3.53	0.77	0.03	0.01	-
16 % Cr White Cast Iron	2.66	0.76	0.03	0.01	-
Ductile Iron	3.5	2.5	0.01	0.01	0.04

Table 3.3 Chemical Composition of Alloying Materials.

Alloying Materials	C %	Si %	S %	Cr %	Mg %
Sorel Pig	4.3	2.0	0.74	0.001	0.005
Scrap	0.08	0.005	0.02	0.02	-
FeCr	0.05	0.86	-	70.0	-
FeSiMg	-	45.0	-	-	5.5

Table 3.4 Chemical Composition of Cerium Mischmetal.

Mischmetal	Ce %	La %	Nd %	Pr %	Sm %	Other Heavies
Cerium Mischmetal	48 – 50	25 – 30	11 – 15	4 – 7	1 – 4	1 – 2

3.2 Mold Design

A specially designed mold in bi-metal casting was used as shown in the Figure 3.1. Two different metals were poured and so two risers were used. The first metal was poured from the first riser up to point 3 and when it solidified up to a critical solid fraction, the second material was poured from the second riser.

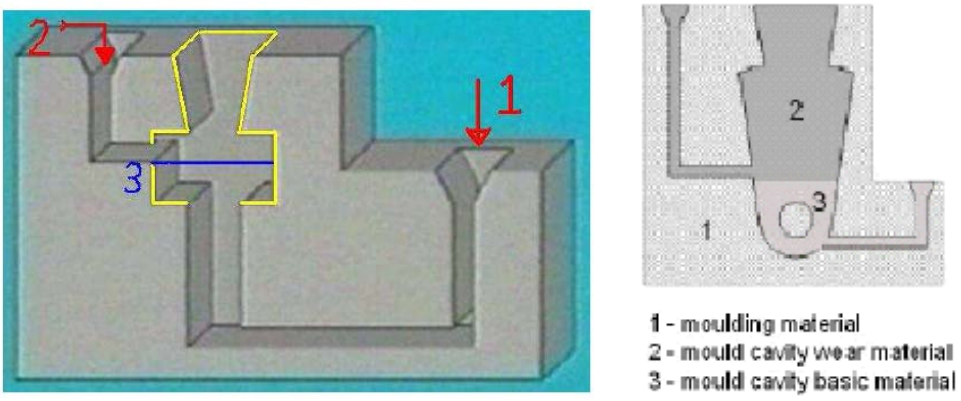

Figure 3.1 Mold Design for Bi-Metal Casting.

The problem in bi-metal casting is the determination of the critical time for pouring the second material. The purpose was to investigate the principal way for producing bi-metals by direct connection of components in liquid state. There must be a critical solid fraction value for the firstly poured metal. To determine this value, cooling curve analysis plays a major role.

Controlling of the interface is the most important part in producing bi-metals. Solid fraction of the firstly poured material, in other words the temperature of it and also the temperature of the second material are the main parameters that affect the structure of the interface. While producing bi-metal, type K thermocouple, low cost and general purpose thermocouple, was put into point 3, where two materials interact, Figure 3.2.

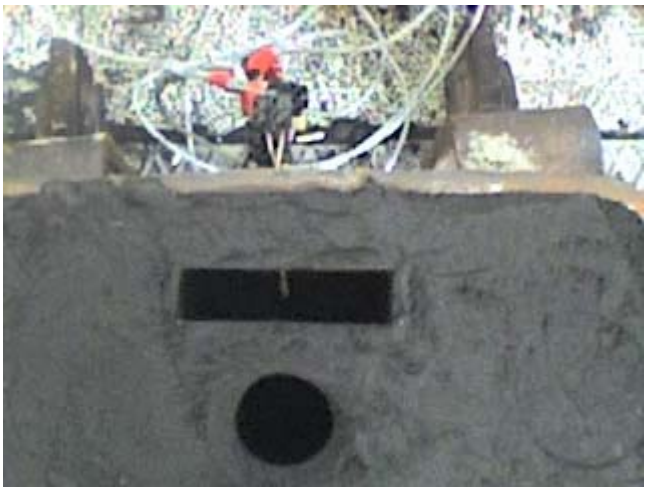

Figure 3.2 Mold Set-Up with Thermocouples.

3.3 Thermal Analysis

Thermal analysis encompasses a family of measurement techniques which record a materials' response to being heated or cooled. Both kinetic and thermodynamic events may be characterized. The dependent variable is usually temperature but may also be time, for example when kinetic processes are being measured [23].

In differential thermal analysis, the thermal analysis experiment consists of the measurement of the sample temperature as a function of time while the sample is either heated or cooled externally. Because the rate of temperature change will

change during phase change, transformations may be detected. In addition, the temperature difference between a reactive sample and a non-reactive reference is determined as a function of time, providing useful information about the temperatures, thermodynamics and kinetics of reactions [23-24].

Thermal analysis is the process of determining the temperature at which phase transformation occurs, a change in the atomic arrangement, by observing the critical temperature such as eutectic temperatures, undercooling temperature, solidus temperature, etc.

Thermal analysis has the potential capability of measuring the course of solidification processes as well as changes in the processes. Solidification process parameters identified and measured by thermal analysis may then be used to evaluate the effects of processing variables on solidification. When cast iron solidifies from the molten state, it passes through several phase changes.

The first phase change is the beginning of primary austenite formation; this is commonly called liquidus. The second phase change represents the end of austenite formation and the beginning of solid state transformation; this is commonly called solidus. Thermal analysis cups attached to a precision instrument, as shown in Figure 3.3, are used to measure these liquidus and solidus values.

Figure 3.3 Thermal Analysis Instrument.

Figure 3.4 Experimental Set-up.

Thermocouples are the most commonly used temperature measuring device in elevated temperature analysis. Thermocouples are made up of two dissimilar metals. If the welded junctions between the two materials are at different temperatures, a current through the loop is generated [24].

By using thermocouples, temperatures were recorded as a function of time for each casting experiment, as shown in Figures 3.4 and 3.5.

Figure 3.5 Recording Temperatures by Elimko Data Acquision System.

3.4 Newtonian Thermal Analysis of Cast Iron

Computer aided cooling curve analysis (CACCA), such as Fourier Thermal Analysis (FTA) and Newton Thermal Analysis (NTA) are valuable tools that give a deeper understanding of the solidification of cast alloys. The interest on these techniques relies on the successful identification of several cooling curve parameters by conventional cooling curve analysis. This allows the prediction of the microstructure of cast products. Another reason is the need to develop more elaborated cooling curve data processing methods in order to gain a better understanding of solidification and a closer control of the melt quality before pouring [25].

Newton Thermal Analysis (NTA) analyzes a cooling curve that is obtained with a thermocouple located at the thermal centre of a cast. NTA calculations are performed on the first derivative of that curve. In the classical version of this method, the times of start and end of solidification are located. The zero baseline curve is obtained from an exponential interpolation between these points. Integration of the area between the cooling curve and the zero baseline curve gives relevant information of the solidification kinetics [25].

3.5 Characterization of Products

Characterization played the vital role in this study. Specimens which were obtained from the experiments were characterized by using spectrometer, metallography, SEM, X-Ray. In addition, their mechanical tests were done such as hardness test, tensile test and toughness test. The results were evaluated by changing experimental conditions. As seen in Figure 3.6, formation, metallurgy and strength of bi-metallic castings and their characterization is very important in this study.

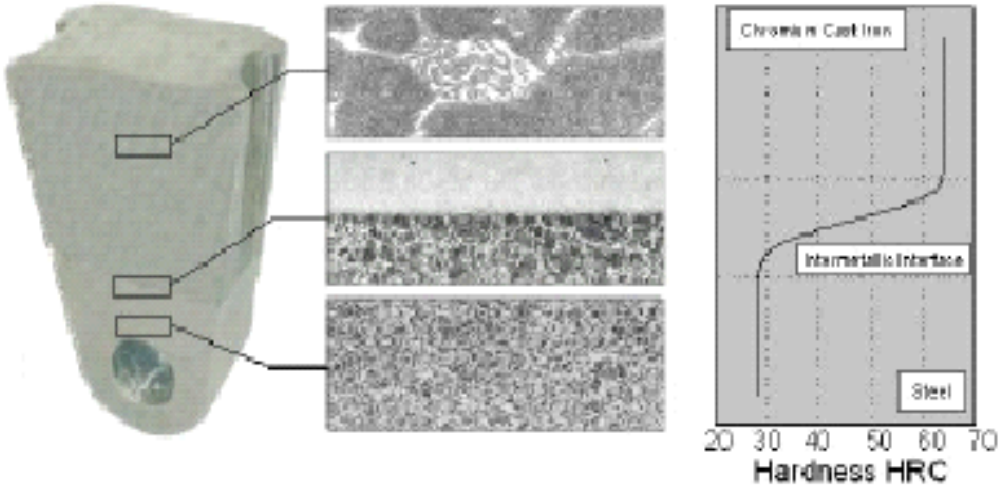

Figure 3.6 Characterization of Bi-Metallic Castings [26].

3.5.1 Metallographic Investigation

Samples were firstly cut and then, they were ground, polished and etched with 2 % Nital. The structures of them were investigated by using optical microscope and photographs were taken by a digital camera.

3.5.2 Scanning Electron Microscopy (SEM Analysis)

By using scanning electron microscope, the detailed and close views of microstructures were evaluated and photographs of them were taken. In addition, energy dispersive X-ray analysis (EDX) was made for different phases.

3.5.3 Hardness Test

Hardness is very important mechanical property in tribosystems. There is a direct relation between hardness and wear rate. Especially in abrasive wear mechanism increase in the hardness value decrease the wear rate of the material. During this study, Brinell and Rockwell hardness test results were used to see the effect of different alloying elements on hardness.

3.5.4 Impact Test

Toughness is the other important mechanical property in tribosystems. Especially in impact wear mechanism, toughness is the most important mechanical property. In some cases both hardness and toughness become the main properties. Charpy impact test was used to see the effects of alloying elements on toughness.

3.5.5 Tensile Test

Tensile test is the general mechanical test to obtain the materials' yield and tensile strength. In addition, the stress and strain diagrams give the general idea about materials' toughness.

In this study, tensile strengths of different cast irons were obtained. Their tensile strenght results were evaluated.

CHAPTER 4

RESULTS AND DISCUSSION

4.1 Failure Analysis of Hadfield Steel Machine Parts

Mining and mineral processing demand wear-resistant machines and components, because the energies and masses of interacting bodies are significant. Impact wear, abrasion and their combinations are the most important cost factors in the areas of mining and mineral processing. The choosen material should have good resistance against impact-abrasive wear and adequate other mechanical properties [27].

The classical coal crusher hammer heads and impact bars are made from Hadfield steels, in other words high manganese austenitic steels. These steels are known as tough materials and they are very useful under impact wear.

Working conditions are very important for Hadfield steels machine parts because the mechanical properties of Hadfield steels are directly dependent on service conditions. Under suitable conditions, Hadfield steel can reach high hardness values and this improvement increases the resistance of the steel to abrasion.

Generally, under severe impact conditions, the hardness values of Hadfield steel machine parts increase by work hardening, in other words by phase transformation from austenite to martensite. The work hardening capability of Hadfield steel plays the major role in this structural change.

According to above informations, it would be logical to see visible structural difference between the used and unused Hadfield steel samples which were taken from Çatalağzı Thermal Power Plant.

4.1.1 Metallographic Investigation

Heat treatment procedure is very important subject in production of Hadfield steel. The matrix should be fully austenite and there must not be any carbides, especially on the grain boundaries.

As seen from Figures 4.1 and 4.2, the unused sample, which was taken from Çatalağzı Thermal Power Plant, is fully austenite and there are no carbides. It is possible to say that, heat treatment of the steel is succesful.

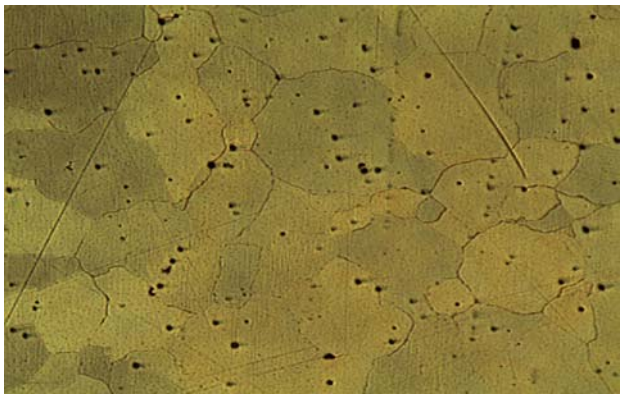

Figure 4.1 Optical Micrograph Showing Unused Hadfield Steel Impact Bar Specimen, 50 X.

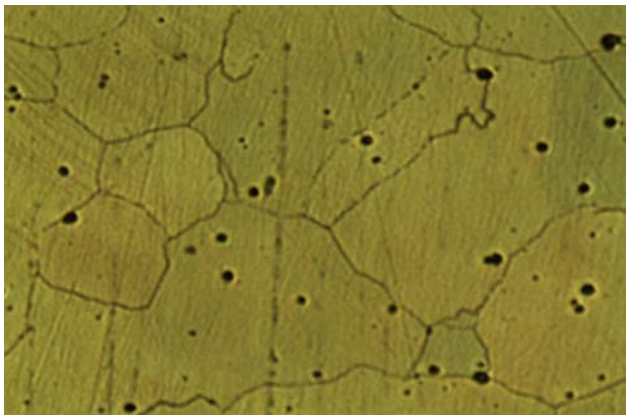

Figure 4.2 Optical Micrograph Showing Unused Hadfield Steel Impact Bar Specimen, 100 X.

Although there is no failure in unused sample, there are microcracks through the grains of the used sample, as can be seen from Figures 4.3 and 4.4.

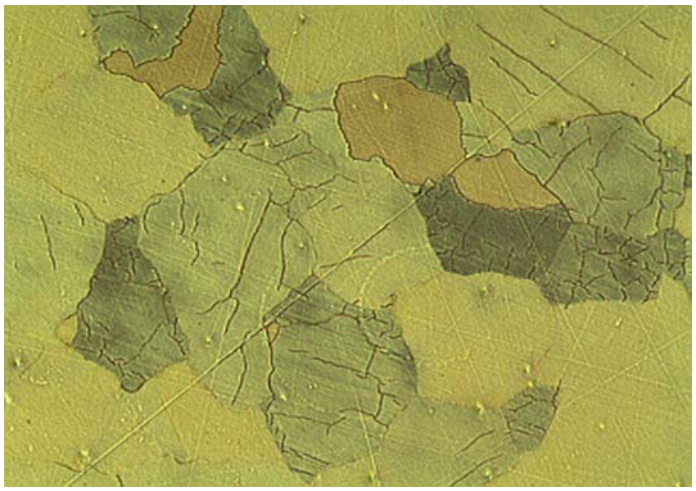

Figure 4.3 Optical Micrograph Showing Used Hadfield Steel Impact Bar Specimen, 50 X.

Figure 4.4 Optical Micrograph Showing Used Hadfield Steel Impact Bar Specimen 100 X.

In addition to these microcracks there is an important degree of wear rate and it results in weight loss.

Abrasive conditions results in the progressive removal of material and due to various phase transformations from austenite to martensite introduces surface volume changes and causes the generation of cracks and further lead the failure of the component [28].

4.1.2 SEM Analysis

Work hardening capability is very high in Hadfield steels. Work hardening occurs by phase transformation from austenite to martensite. Thus, mechanical properties, such as hardness increases in Hadfield steels by time. Although some parts of Hadfield steel scrap are fully martensite, as shown in Figure 4.5, martensitic transformation is not complete yet, as seen from Figure 4.6.

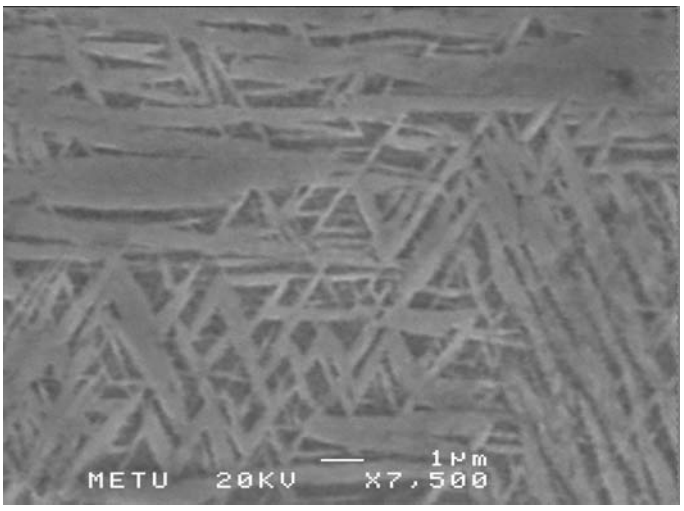

Figure 4.5 SEM Micrograph of Used Hadfield Steel Impact Bar Specimen, 7500 X.

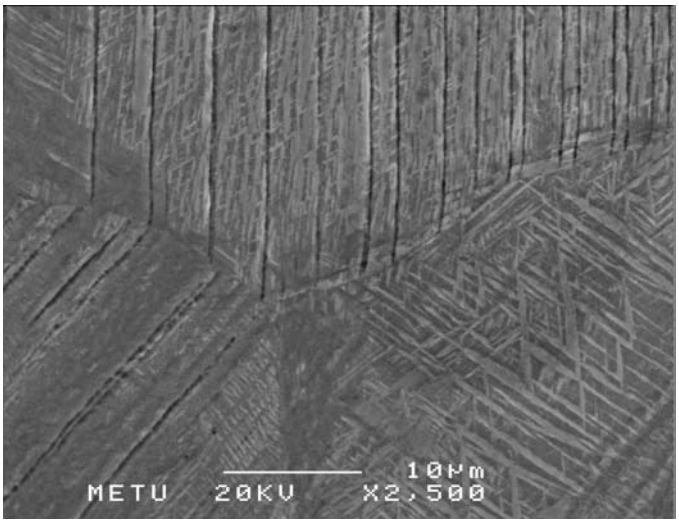

Figure 4.6 SEM Micrograph of Used Hadfield Steel Impact Bar Specimen, 2500 X.

In addition, as seen from Figure 4.7, the austenitic grain is clear. Although the sample is scrap, there are still austenitic grains and it means that the service conditions are not suitable for Hadfield steel to complete the phase transformation.

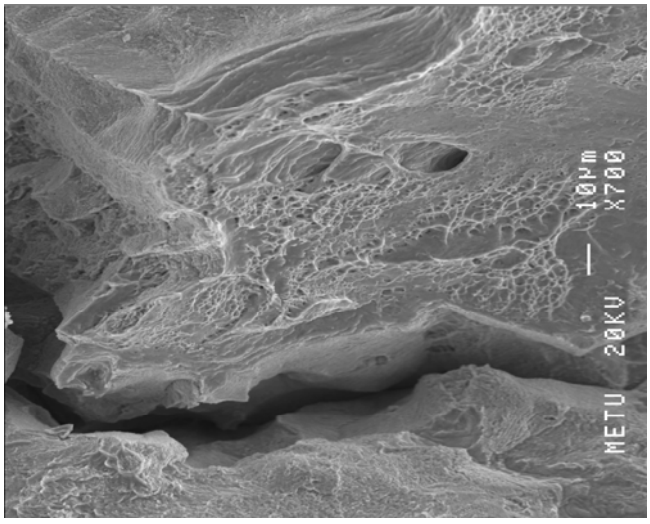

Figure 4.7 SEM Micrograph of Used Hadfield Steel Impact Bar Specimen, 7000 X.

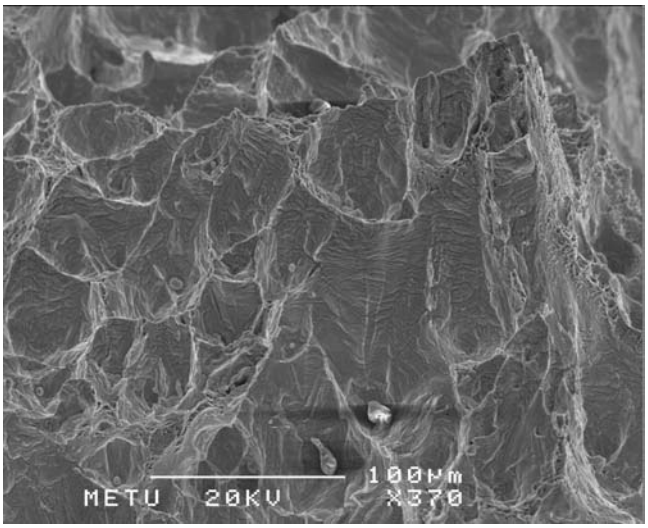

Figure 4.8 SEM Micrograph of Used Hadfield Steel Impact Bar Specimen, 3700 X.

Examinations indicated the presence of combined ductile (dimpled), as shown in Figure 4.8 and brittle fracture on the cracked surfaces. This is judged to be the result of transformation of austenite to martensite, probably induced by high compressive surface stresses [28].

Degradation of power plant components is mainly due to abrasion by quartz and alumino-silicates that are in the coal. In addition to material composition, the service conditions also play a significant role in degradation of the components. Material properties such as hardness, fracture toughness and microstructure also play a significant role in degradation of material and/or material removal due to interactions with abrading media such as the silica/coal particles [28-29].

4.2 Experiments of Bi-metal Production for Unalloyed Cast Irons

At the first part of the bi-metal production experiments, unalloyed white cast iron as a wear resistant material and grey cast iron as a tough material were examined. The aim is to determine the best solid fraction range for pouring the second material and apply this results to alloyed material casting applications.

4.2.1 Initial Experiment

The initial bi-metal production experiment showed that, there must be a critical time to pour the second material. At this experiment, white cast iron was firstly poured into the mold and 60 seconds later the second material, grey iron, was poured.

Figure 4.9 Photograph of Initial Bi-Metal Experiment Product.

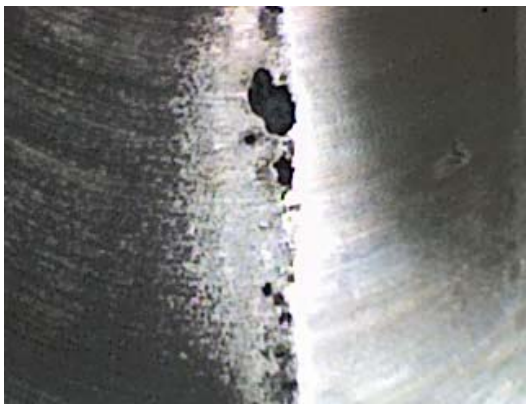

Figure 4.10 Photograph of Initial Bi-Metal Interface.

As seen from Figures 4.9 and 4.10, there is not a good combination between two materials and there is a porous interface which is very brittle. According to this

initial experiment results, it was determined that, starting point had to be thermal analysis of each material and then bi-metal would be produced.

4.2.2 Thermal Analysis

As stated from the previous chapters, thermal analysis is an important tool in this study. The cooling curves give important informations about materials' characters while solidifying.

Figures 4.11 and 4.12 are the cooling curves of unalloyed white cast iron and grey cast iron.

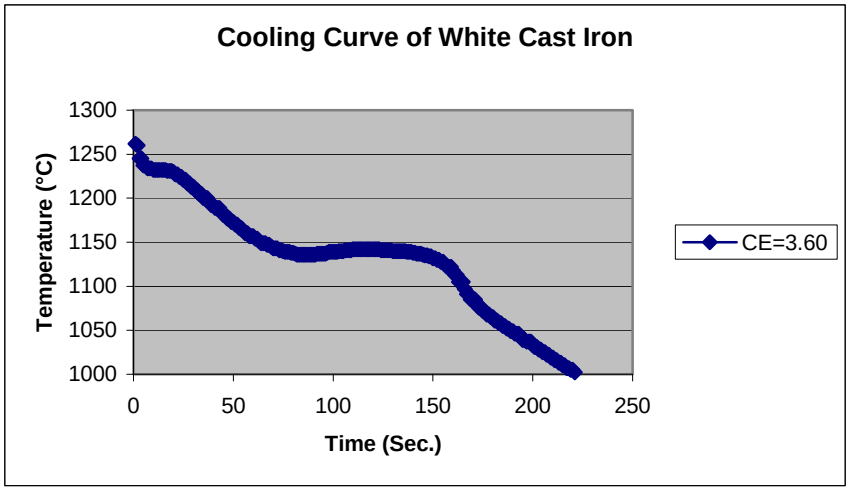

Figure 4.11 Cooling Curve of Unalloyed White Cast Iron.

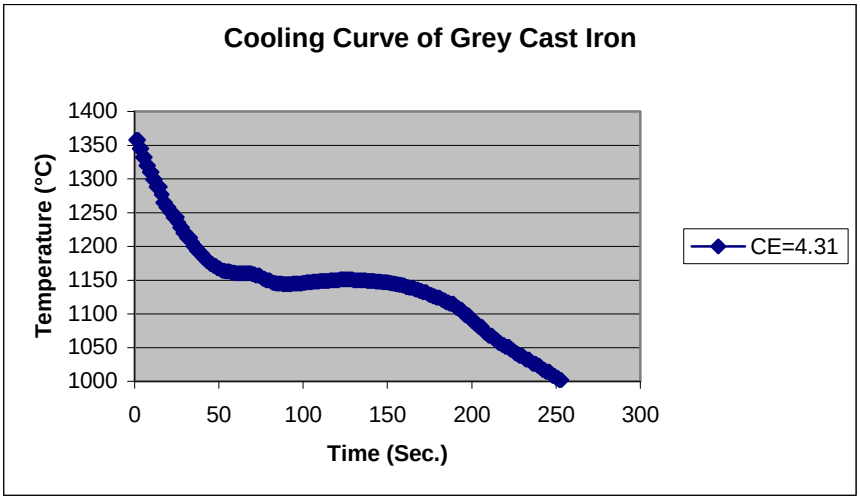

Figure 4.12 Cooling Curve of Unalloyed Grey Cast Iron.

From the Figures 4.11 and 4.12, the eutectic temperatures are 1140 °C and 1150 °C for white and grey irons. These temperatures which decrease by time gave us the solid fraction values by using Newtonian Thermal Analysis as discussed previous chapter, Figures 4.13, 4.14, 4.15, 4.16.

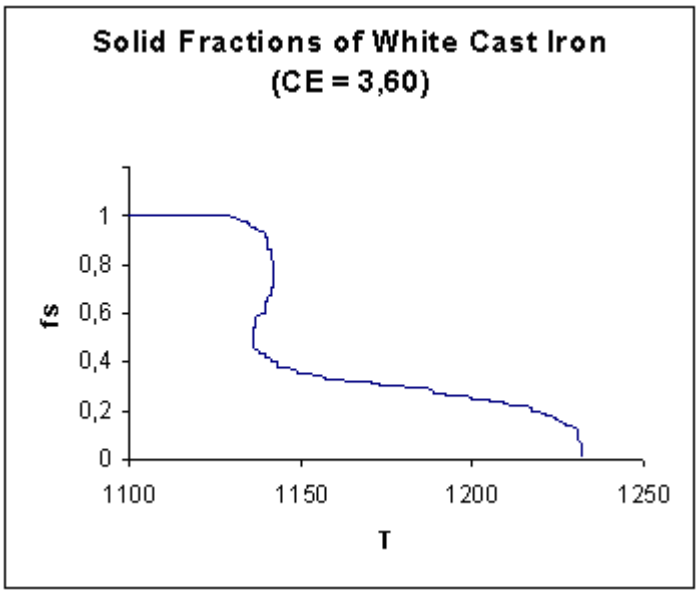

Figure 4.13 Solid Fractions of White Cast Iron by Temperature (°C).

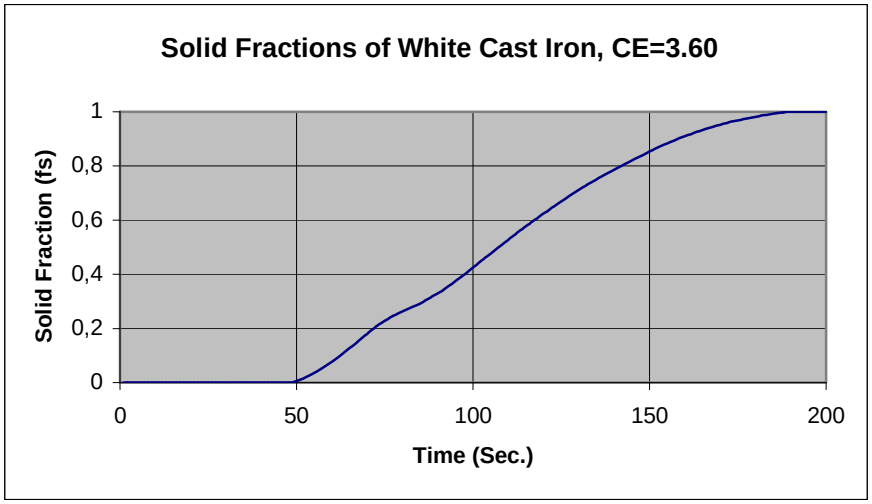

Figure 4.14 Solid Fractions of White Cast Iron by Time (Sec.).

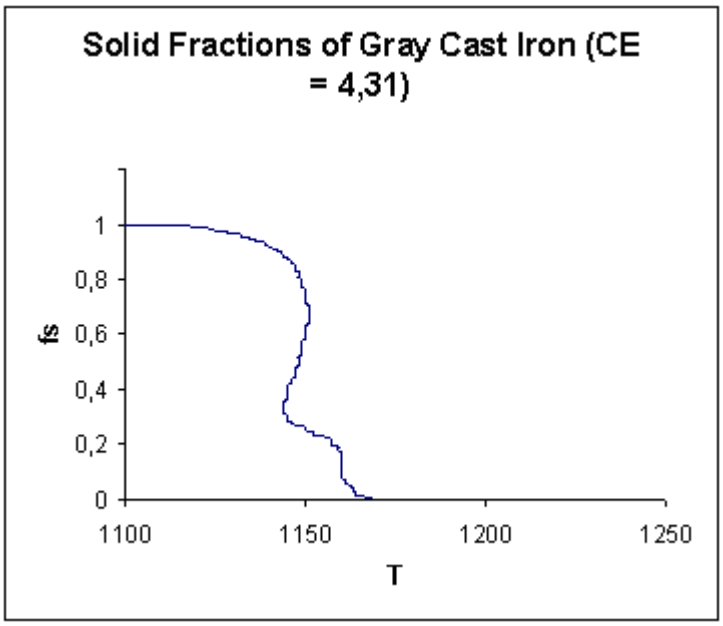

Figure 4.15 Solid Fractions of Grey Cast Iron by Temperature (°C).

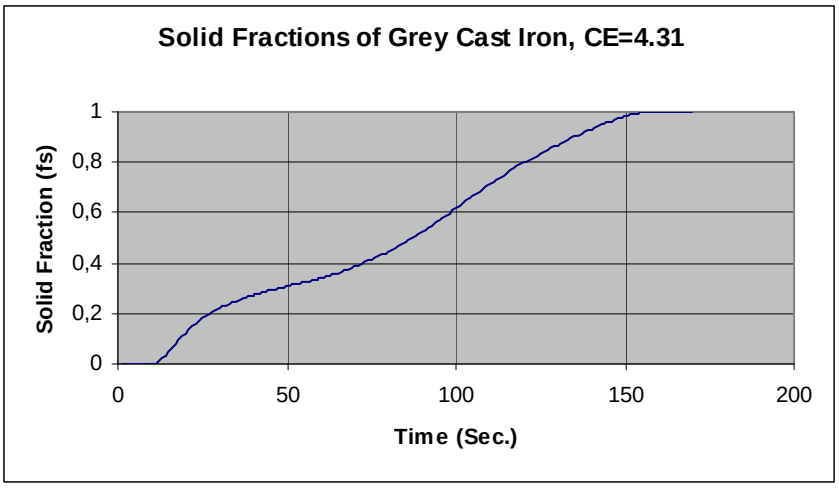

Figure 4.16 Solid Fractions of Grey Cast Iron by Time (Sec.).

By using these graphs, the solid fractions by temperature and by time can be controlled. During the bi-metal producing experiment these graphs became a useful tool.

4.2.3 Evaluation of Following Experiments

1) Firstly, the white cast iron was poured and waited until the temperature decrease to 1150 °C. Then, the grey cast iron was poured at 1400 °C. 1150 °C corresponds 36.5 % solid fraction for white cast iron.

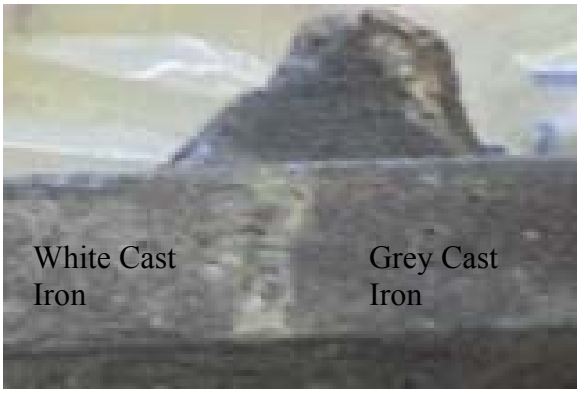

Figure 4.17 Photograph of Bi-Metal Experiment Product at 36.5 % Solid Fraction.

As compared with the initial experiment, it is seen from Figure 4.9, the combination of two materials is better and there is no porous interface as shown in Figure 4.17.

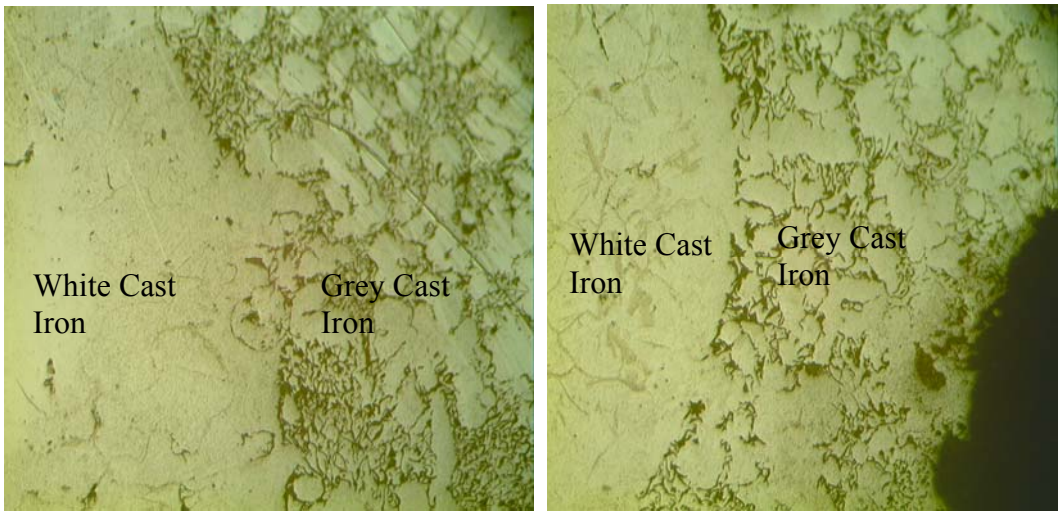

Figure 4.18 Optical Micrograph Showing the Interface Between Grey and White Cast Iron, 36.5 % Solid Fraction, 100 X.

It is also seen from Figures 4.18 and 4.19 that there is a smooth interface.

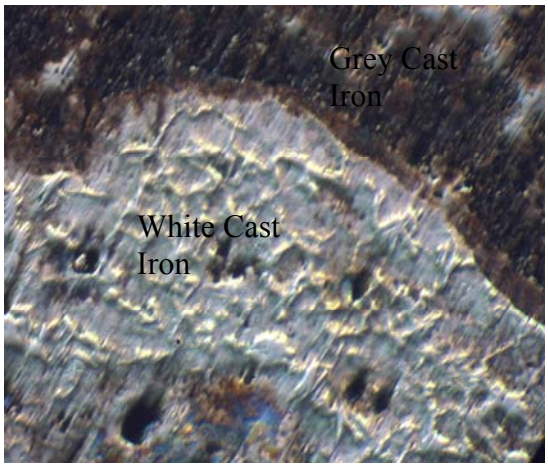

Figure 4.19 Optical Micrograph Showing the Interface Between Grey and White Cast Iron, Etched with 2 % Nital, 100 X.

The microstructure which was etched with 2% Nital, shows the interface more clear. But it is also seen that there is no transition between two materials and this does not give permission to interface to the become a suitable transition phase between two materials.

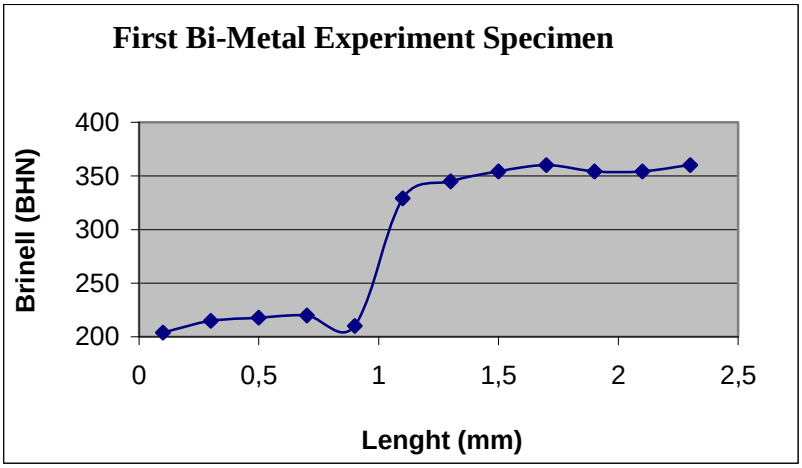

Figure 4.20 Hardness Transition of Bi-Metal Experiment Specimen 1.

2) Secondly, the white cast iron was poured and waited until the temperature decreased to 1180 °C. Then, the grey cast iron was poured at 1400 °C. 1180 °C corresponds to 29.4 % solid fraction for white cast iron.

Figure 4.21 Photograph of Bi-Metal Experiment Product at 29.4 % Solid Fraction.

The interface is satisfactory, there are no cracks and pores on the interface, as shown in Figures 4.21 and 4.22.

Figure 4.22 Optical Micrograph Showing the Interface Between Grey and White Cast Iron, 29.4 % Solid Fraction, 100 X.

From the metallographic investigations, it is seen that the interface is smooth but there are some transition regions between two materials. Decreasing the solid fraction from 36.5 % to 29.4 % let the transition between two materials.

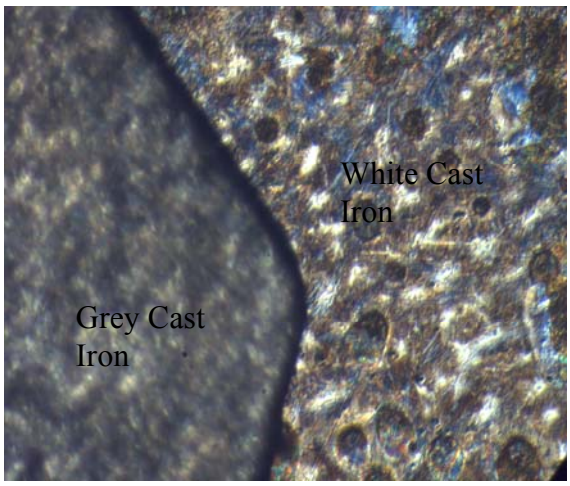

Figure 4.23 Optical Micrograph Showing the Interface Between Grey and White Cast Iron, Etched with 2 % Nital, 100 X.

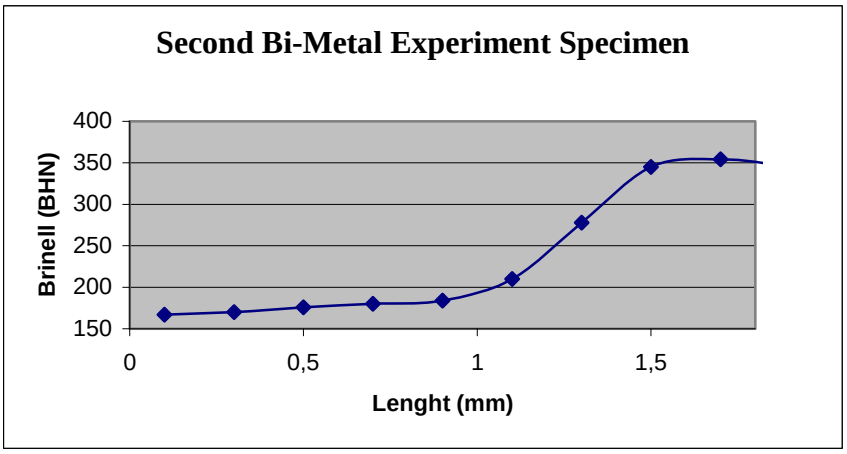

Figure 4.24 Hardness Transition of Bi-Metal Experiment, Specimen 2.

Hardness transition is significant in bi-metals. The hardness transition must be gradual. The hardness of the interface should have the value between two materials. As shown in Figure 4.24, the hardness increases gradually along length.

3) For the third bi-metal production experiment, grey cast iron was poured firstly. When the temperature decreased to 1150 °C, the white cast iron was poured at 1400 °C. 1150 °C corresponds 25 % solid fraction for grey cast iron.

Figure 4.25 Photograph of Bi-Metal Experiment Product at 25 % Solid Fraction, Macroetched with 10 % Nital.

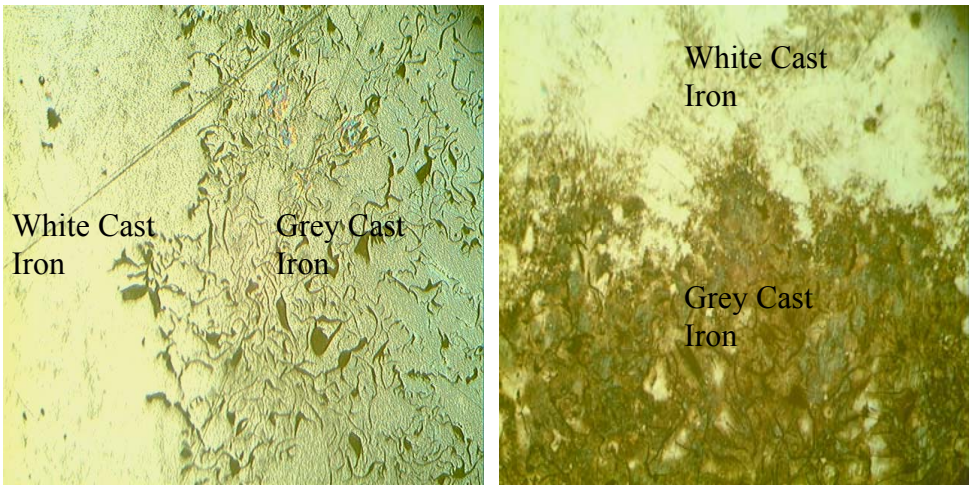

Figure 4.26 Optical Micrograph Showing the Interface Between Grey and White Cast Iron, 25 % solid fraction, 100 X.

The microstructures show that when the solid fraction decreases, transition between two materials increases. In this experiment, the solid fraction of the firstly poured metal was 25 % , the lowest ratio, the transition is also more clear.

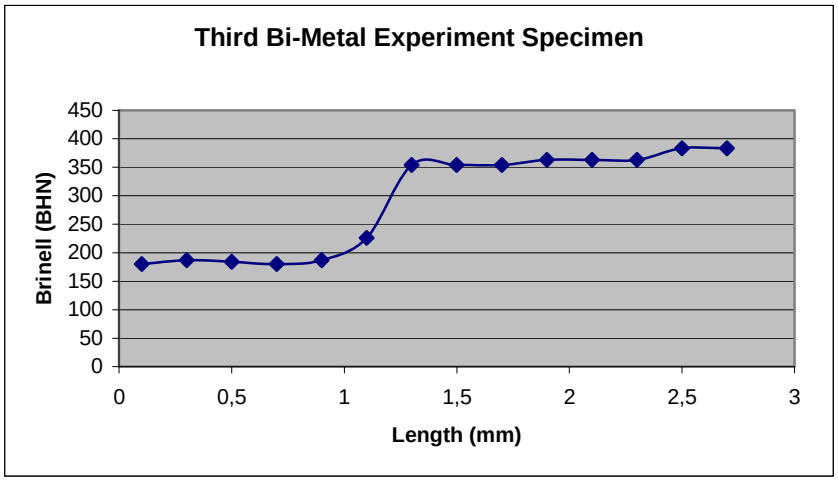

Figure 4.27 Hardness Transition of Bi-Metal Experiment, Specimen 3.

4.3 Experiments of Bi-metal Production for Alloyed Cast Irons

At the second part of the bi-metal production experiments, high chromium white cast iron as a wear resistant material and ductile iron as a tough material were examined. By using the results which were taken from the first part of the experiments used for alloyed cast irons and analized.

4.3.1 Experiments of High Chromium White Cast Iron

As mentioned in Chapter 2, high chromium white cast iron is widely used as a wear resistant material. By changing chromium ratio, the properties of iron also change. In the following experiments, the high chromium white cast iron was investigated with different chromium contents. Three different chromium contents, 5 %, 10 % and 16 % were added to white cast iron and their metallographic, thermal, hardness and SEM investigations were made.

4.3.1.1 5 % Chromium White Cast Iron

The first alloy is 5 % Cr white cast iron. At first, Sorel pig and low carbon steel scrap were melted and ferrochromium (70 % Cr) was added as an alloying material. Charge calculation was made before casting to obtain 5 % Cr white cast iron.

Table 4.1 Chemical Composition of 5 % Chromium White Cast Iron.

Chromium White Cast Iron	C %	Si %	P %	S %
5 % Cr White Cast Iron	3.78	0.78	0.053	0.015

By using a thermal analysis quick cup, cooling curve of 5 % Cr white cast iron was obtained, as given in Figure 4.28 .

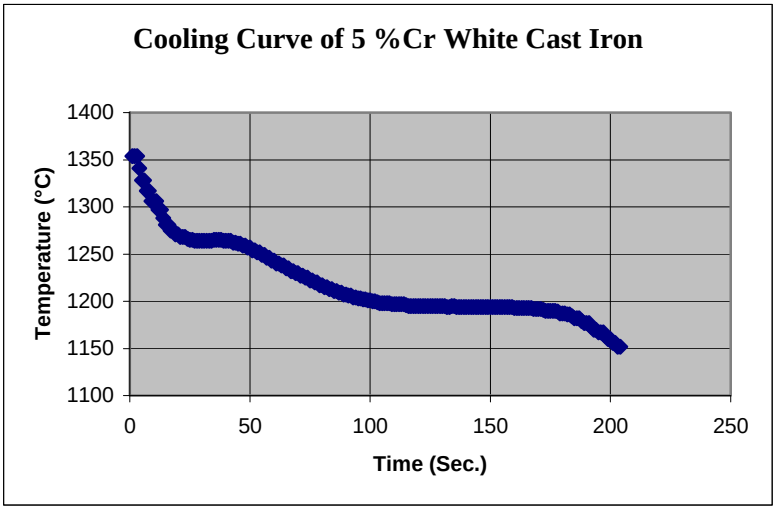

Figure 4.28 Cooling Curve of 5 % Cr White Cast Iron.

From the cooling curve, eutectic temperature of 5 % Cr white cast iron is about 1200 °C.

For metallographic investigation, the specimens were prepared and photographs of microstructures were taken by using an optical microscope with digital camera, Figure 4.29 .

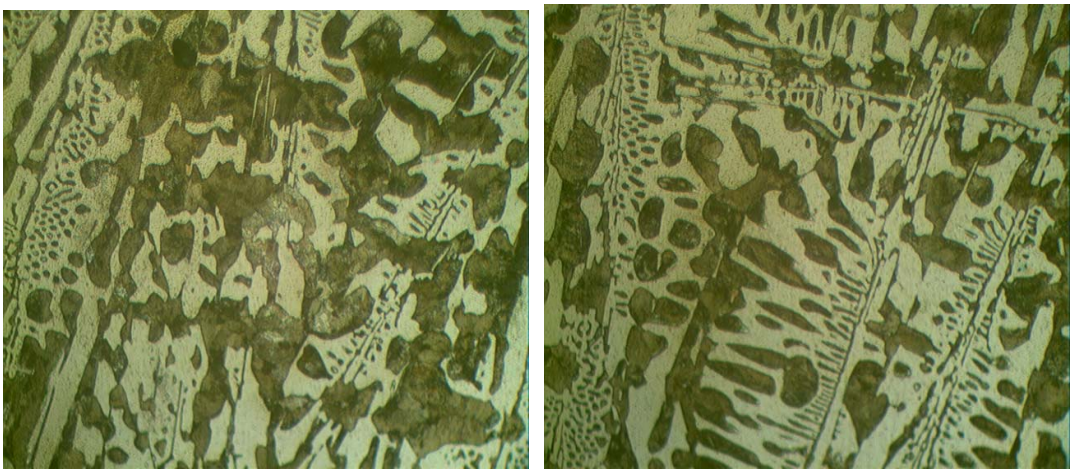

Figure 4.29 Optical Micrograph Showing 5 % Cr White Cast Iron, 400 X.

As seen from Figure 4.29, **t**he white phases are chromium carbides. The matrix also consists of dendrites of austenite, some of which may have transformed into martensite [13]. The main aim for chromium addition to iron is chromium carbide formation to obtain high hardness values.

4.3.1.2 10 % Chromium White Cast Iron

The second alloy is 10 % Cr white cast iron. At first, Sorel pig and low carbon steel scrap were melted and ferrochromium (70 % Cr) was added as an alloying material. Charge calculation was made before casting to obtain 10% Cr white cast iron, as shown in Table 4.2.

Table 4.2 Chemical Composition of 10 % Chromium White Cast Iron.

Chromium White Cast Iron	C %	Si %	P %	S %
10 % Cr White Cast Iron	3.78	0.78	0.053	0.015

By using a thermal analysis quick cup, cooling curve was obtained, Figure 4.30 .

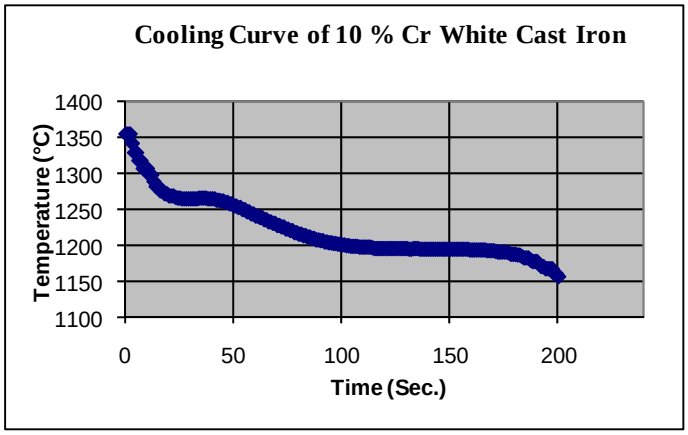

Figure 4.30 Cooling Curve of 10 % Cr White Cast Iron.

From the cooling curve, eutectic temperature of 10 % Cr white cast iron is about 1200 °C.

For metallographic investigation, the specimens were prepared and photographs of microstructures were taken by using an optical microscope with digital camera.

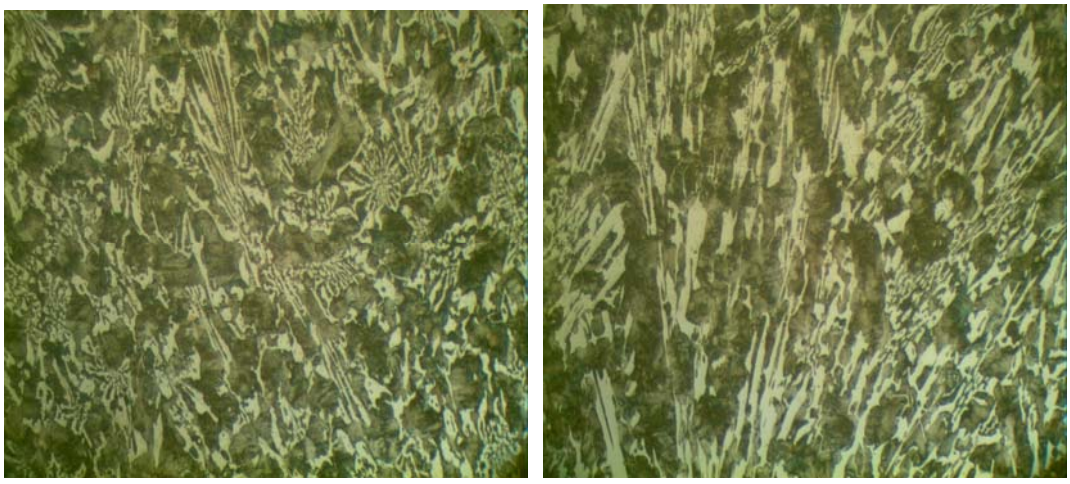

Figure 4.31 Optical Micrograph Showing 10 % Cr White Cast Iron, 400 X.

By increasing the chromium content, the volume of the chromium-rich carbides and hardness also increases up to a limit.

As seen from the microstructures, Figure 4.31, the shapes of chromium carbides in the 10 % Cr are different from 5 % Cr white cast iron.

By using scanning electron microscope, the detailed and close views of microstructures were evaluated and photographs of them were taken. In addition Figures 4.32 and 4.33, energy dispersive X-ray analysis (EDX) was made for different phases.

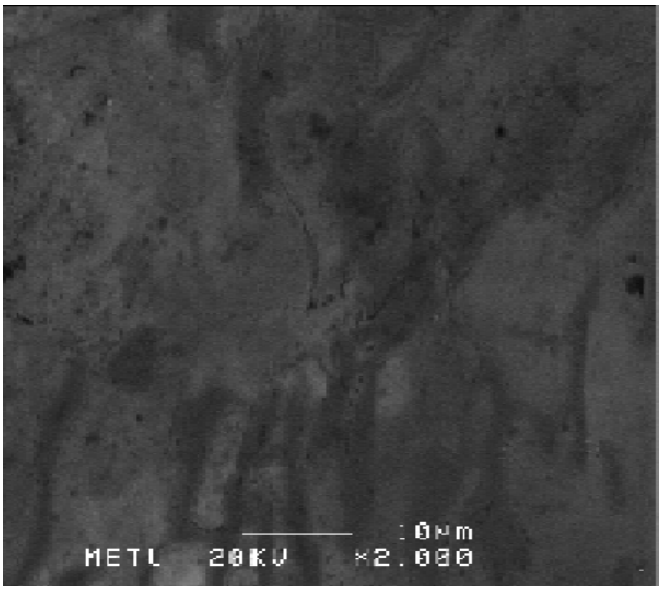

Figure 4.32 SEM Micrograph (Back Scattered) of 10 % Cr White Cast Iron, 2000 X.

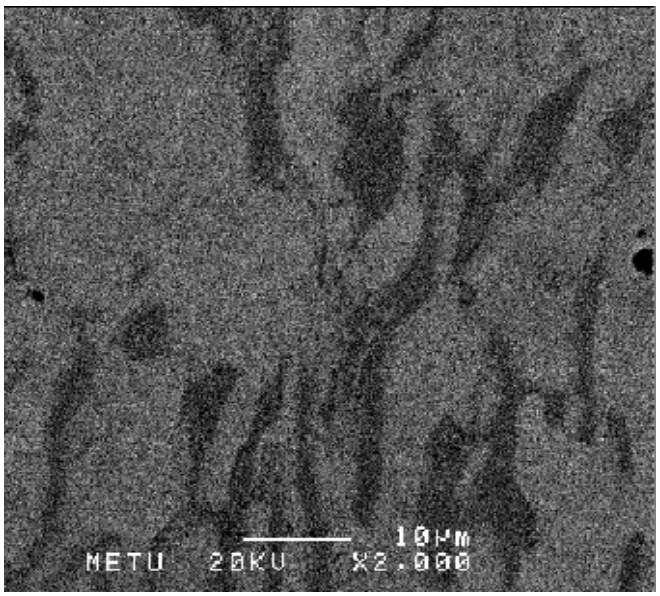

Figure 4.33 SEM Micrograph of 10 % Cr White Cast Iron, 2000 X.

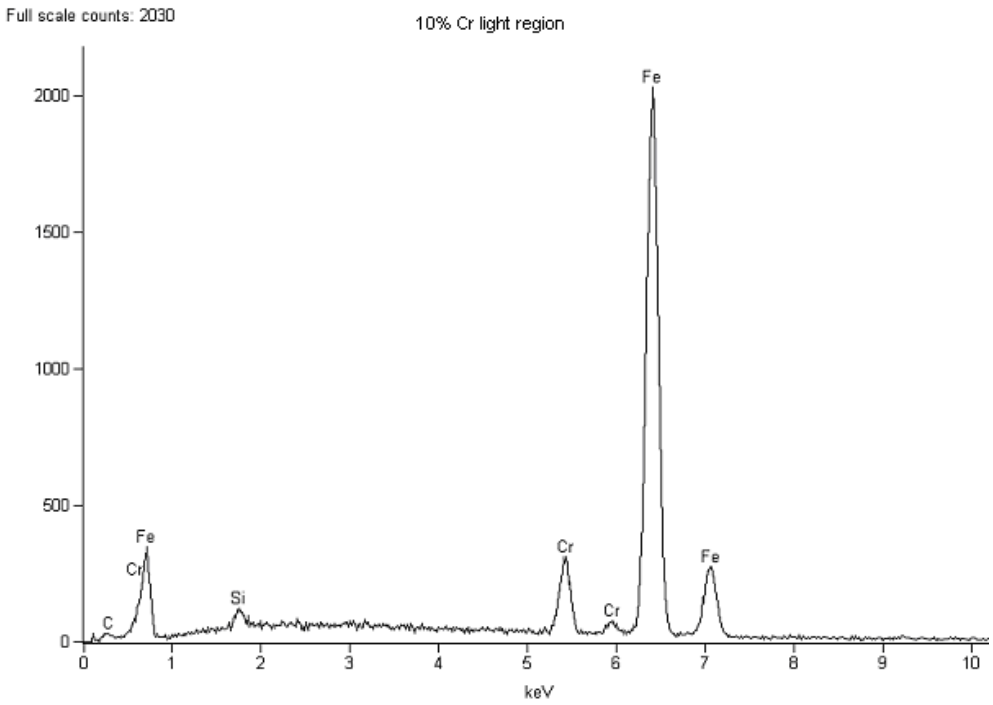

Table 4.3 EDX Analysis of 10 % Chromium White Cast Iron, Light Region.

Element	*Weight Conc %*	*Atom Conc %*
Si	1.17	2.28
Cr	7.09	7.49
Fe	91.74	90.23

From the EDX analysis, Table 4.3, the iron content is about 90 % and it was understood that these regions are main matrix.

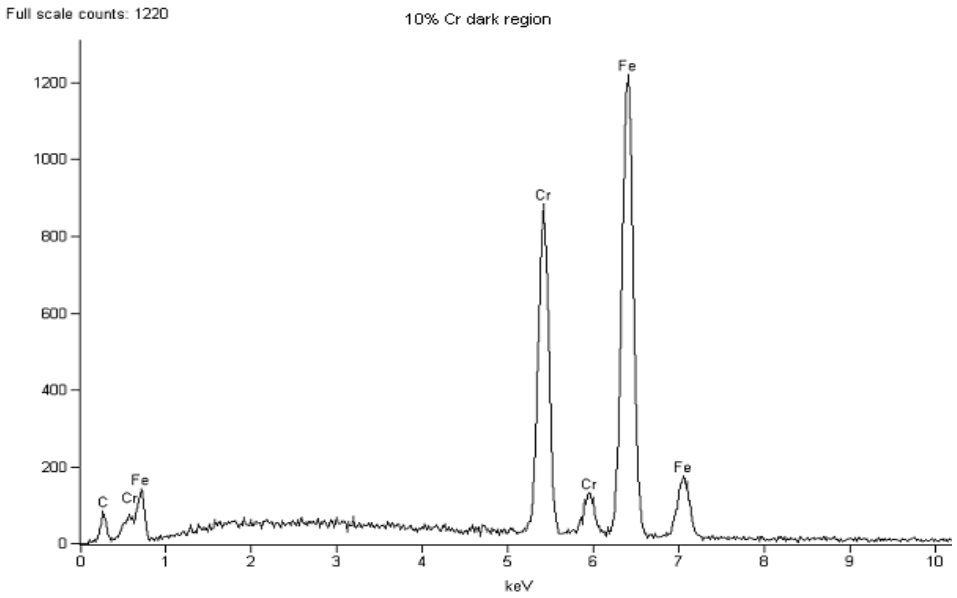

Table 4.4 EDX Analysis of 10 % Chromium White Cast Iron, Dark Region.

Element	*Weight Conc %*	*Atom Conc %*
C	28.10	63.98
Cr	22.20	11.67
Fe	49.71	24.34

As seen from the EDX analysis of the dark regions of microstructure, the chromium content and carbon content are very high, in addition the iron content is about 25 % which was 90 % in the matrix. These regions are chromium carbides and they provide high hardness and increase abrasive wear resistance.

4.3.1.3 16 % Chromium White Cast Iron

The third alloy is 16 % Cr white cast iron. At first, Sorel pig and low carbon steel scrap were melted and ferrochromium (70 % Cr) was added as an alloying material. Charge calculation was made before casting to obtain 16 % Cr white cast iron.

Table 4.5 Chemical Composition of 10 % Chromium White Cast Iron.

Chromium White Cast Iron	C %	Si %	P %	S %
16 % Cr White Cast Iron	2.66	0.76	0.03	0.01

By using a thermal analysis quick cup, cooling curve was obtained, Figure 4.34.

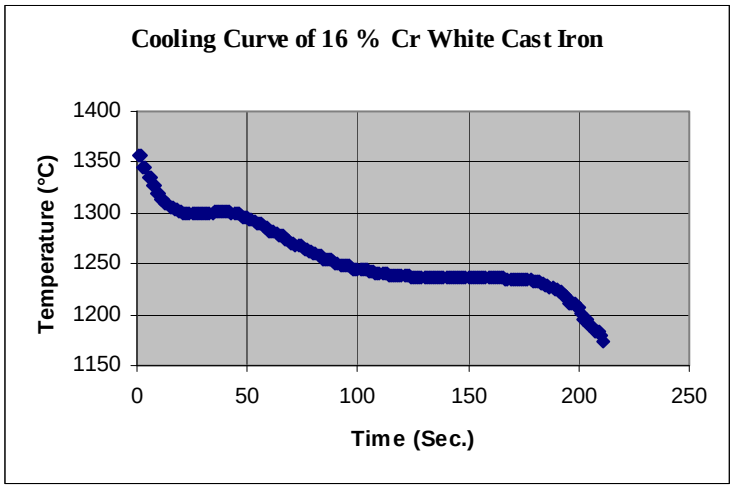

Figure 4.34 Cooling Curve of 16 % Cr White Cast Iron.

From the cooling curve, eutectic temperature of 16 % Cr white cast iron is about 1230 °C.

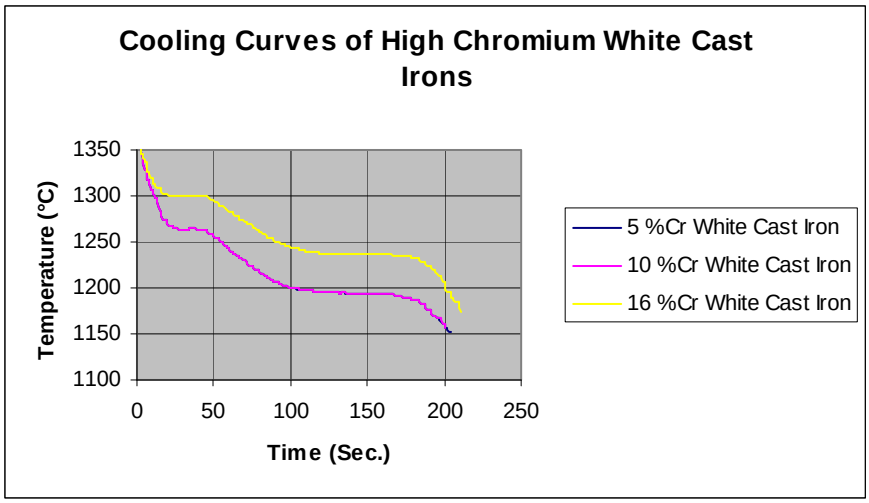

Figure 4.35 Cooling Curves of High Chromium White Cast Irons.

As shown in Figure 4.35, eutectic temperature of 16 % Cr white cast iron is higher than 5 % Cr and 10 % Cr white cast irons, whereas 5 % Cr and 10 % Cr white cast irons have same eutectic temperatures.

For metallographic investigation, the specimens were prepared and photographs of microstructures were taken by using an optical microscope with digital camera, as shown in Figure 4.36.

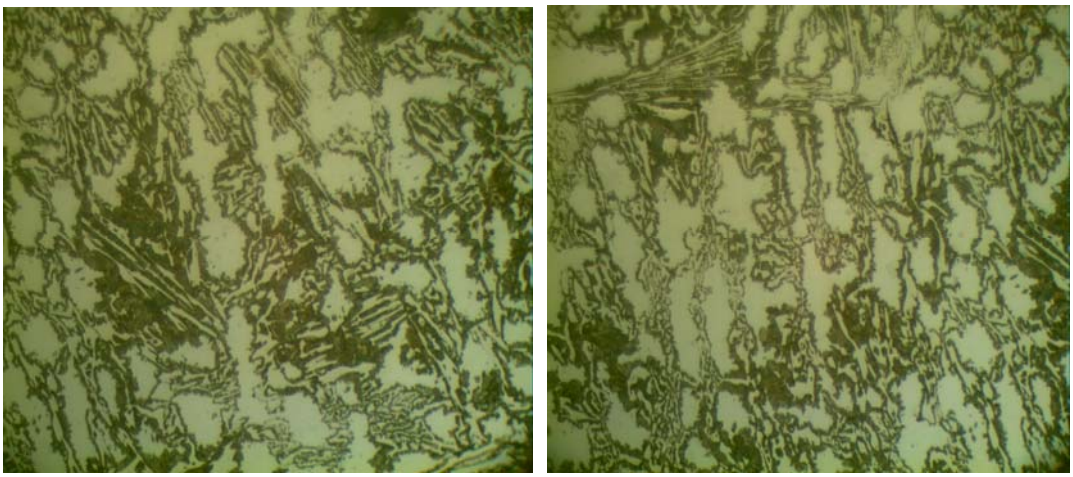

Figure 4.36 Optical Micrograph Showing 16 % Cr White Cast Iron, 400 X

By increasing chromium content, chromium carbides became more clear. The chromium carbides started to widen and formed the white regions by increasing the chromium content.

By using scanning electron microscope, the detailed and close views of microstructures were evaluated and photographs of them were taken. In addition, energy dispersive X-ray analysis (EDX) was made for different phases, as shown in Figures 4.37 and 4.38.

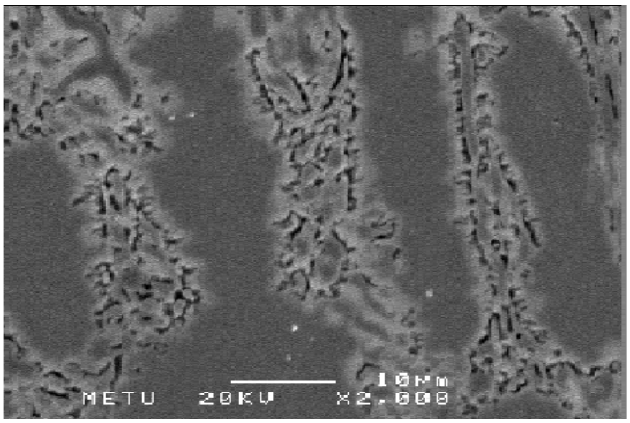

Figure 4.37 SEM Micrograph (Back Scattered) of 16 % Cr White Cast Iron, 2000 X .

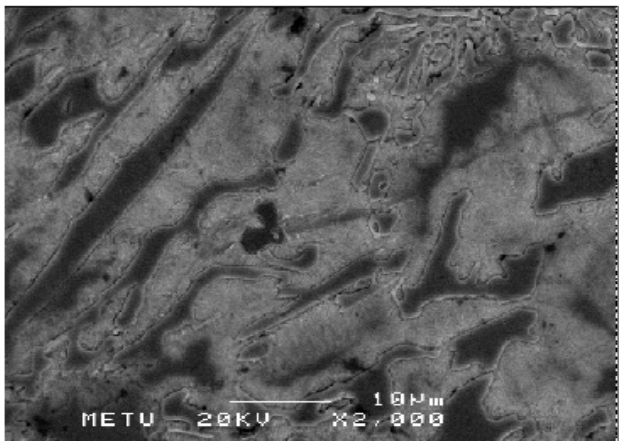

Figure 4.38 SEM Micrograph of 16 % Cr White Cast Iron, 2000 X.

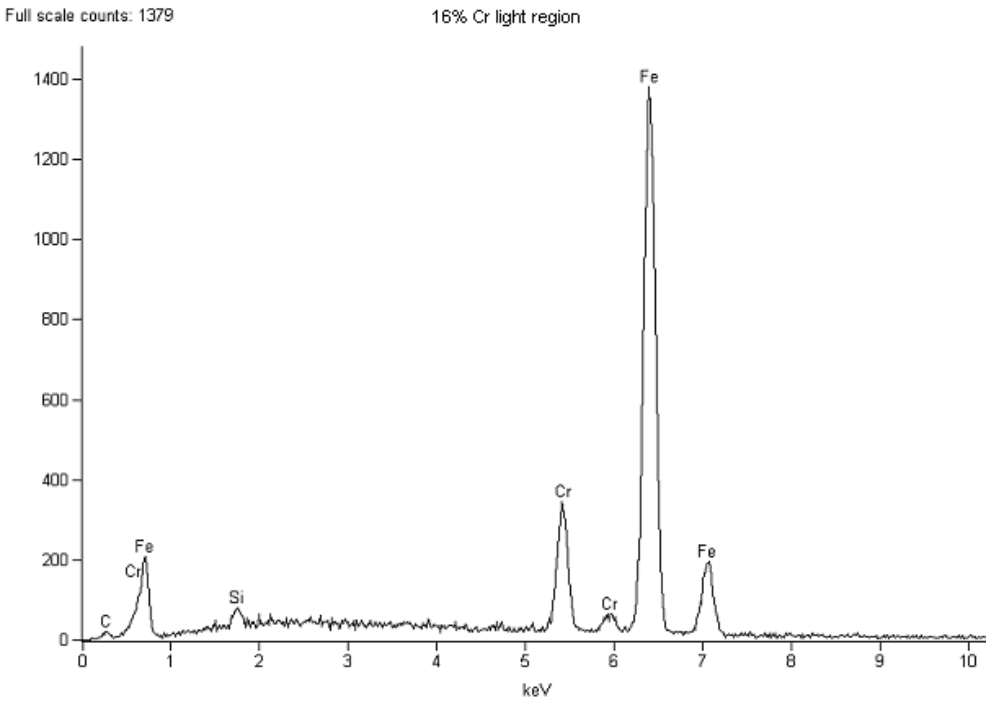

Table 4.6 EDX Analysis of 16 % Chromium White Cast Iron, Light Region.

Element	*Weight Conc %*	*Atom Conc %*
Si	1.23	2.39
Cr	12.31	12.94
Fe	86.47	84.67

From the EDX analysis, Table 4.6, the iron content is about 85 % and it was understood that these regions are main matrix.

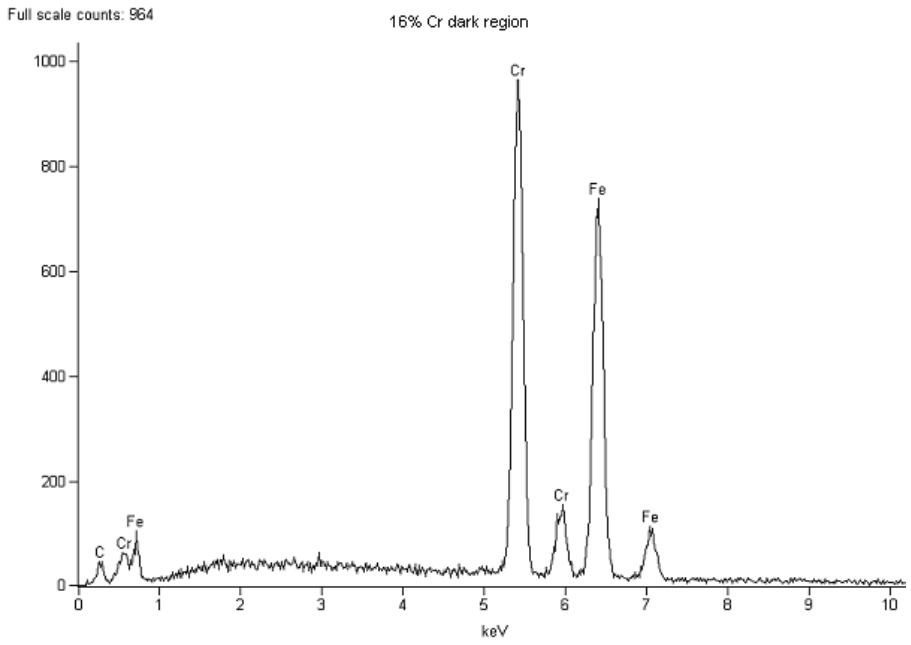

Table 4.7 EDX Analysis of 16 % Chromium White Cast Iron, Dark Region.

Element	*Weight Conc %*	*Atom Conc %*
Cr	47.48	49.26
Fe	52.52	50.74

As seen from the EDX analysis of the dark regions of microstructure, the chromium content is very high, in addition the iron content is about 50 % which was 85 % in the matrix. These regions are chromium-rich carbides and they provide high hardness and increase abrasive wear resistance.

4.3.2 Experiments with Ductile Iron

As mentioned in Chapter 2, in this material the graphite is nodular in form in the as-cast state and the tensile strength is considerably higher than that of grey iron and the impact resistance is much greater [12] .

4.3.2.1 Experiment 1

Firstly, Sorel pig and low carbon steel scrap were melted in induction furnace and FeSi was added as ferroalloy. Secondly, magnesium treatment was made. At this stage, the aim was provide the Mg / S ratio higher than 7. Thus, Mg was added to molten iron as FeSiMg (5.5 % Mg), assuming that magnesium recovery is 33 % . The last step was inoculation. For inoculation, 0.5 % of the total charge FeSi powder was added to the melt before pouring.

Table 4.8 Chemical Composition of Ductile Iron, Experiment 1.

Ductile Iron	C %	Si %	P %	S %	Mg %
Experiment 1	2.70	3.60	0.05	0.02	0.01

By using a thermal analysis quick cup, cooling curve was obtained,

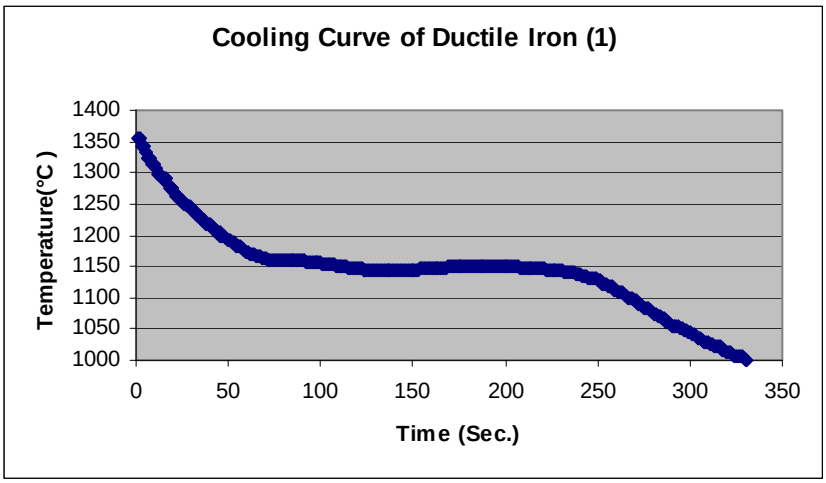

Figure 4.39 Cooling Curve of Ductile Iron (1).

From the cooling curve, Figure 4.39, eutectic temperature of Ductile Iron (1) is about 1150 °C.

For metallographic investigation, the specimens were prepared and photographs of microstructures were taken by using an optical microscope with digital camera, as shown in Figures 4.40, 4.41, 4.42 and 4.43.

Figure 4.40 Optical Micrograph Showing Ductile Iron (1) Iron, 200 X.

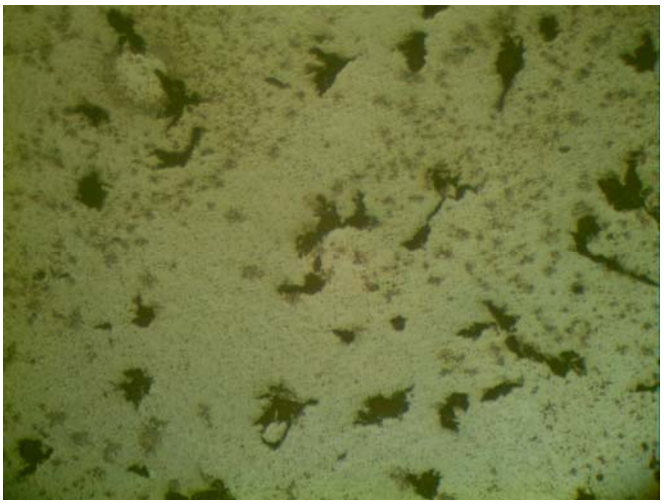

Figure 4.41 Optical Micrograph Showing Ductile Iron (1) Iron, 400 X.

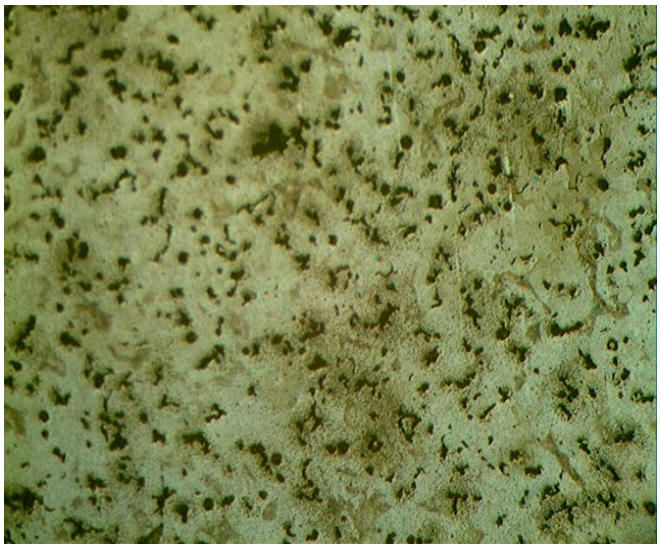

Figure 4.42 Optical Micrograph Showing Ductile Iron (1) Iron, Etched with 2 % Nital, 200 X.

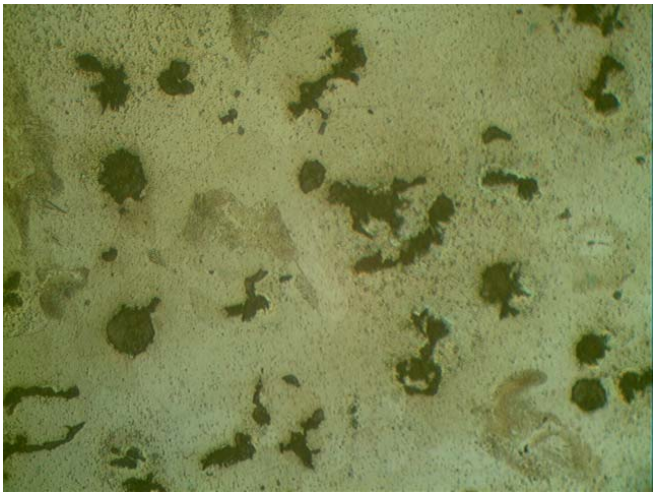

Figure 4.43 Optical Micrograph Showing Ductile Iron (1) Iron, Etched with 2 % Nital, 400 X.

The shape of the nodules are not satisfactory. There are some parameters that affect the nodules, such as Mg / S ratio, the efficiency of inoculation, the process time, especially the time of the magnesium treatment process.

As shown in Figure 4.43, it can be said that shapes of graphites are failed.

4.3.2.2 Experiment 2

Firstly, Sorel pig and low carbon steel scrap were melted in induction furnace and FeSi was added as ferroalloy. Secondly, magnesium treatment was made. At this stage, the aim was to obtain the Mg / S ratio higher than 7. Thus, Mg was added to molten iron as FeSiMg (5.5 % Mg) assuming that magnesium recovery is 33 % . The last step was inoculation. For inoculation, 0.5 % of the total charge FeSi powder was added to the melt before pouring.

Table 4.9 Chemical Composition of Ductile Iron, Experiment 2.

Ductile Iron	C %	Si %	P %	S %	Mg %
Experiment 2	3.5	2.5	0.01	0.01	0.04

By using a thermal analysis quick cup, cooling curve was obtained, as shown in Figure 4.44.

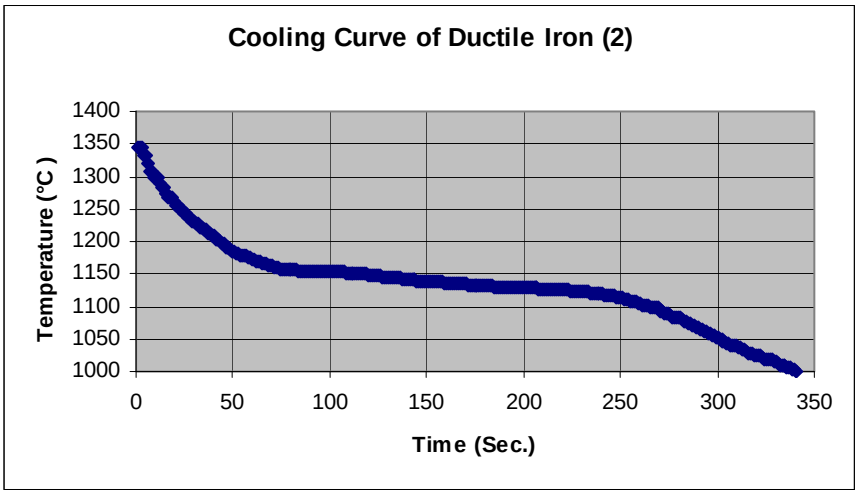

Figure 4.44 Cooling Curve of Ductile Iron (2).

From the cooling curve, Figure 4.44, eutectic temperature of ductile iron is about 1150 °C.

For metallographic investigation, the specimens were prepared and photographs of microstructures were taken by using an optical microscope with digital camera, as shown in Figures 4.45, 4.46 and 4.47.

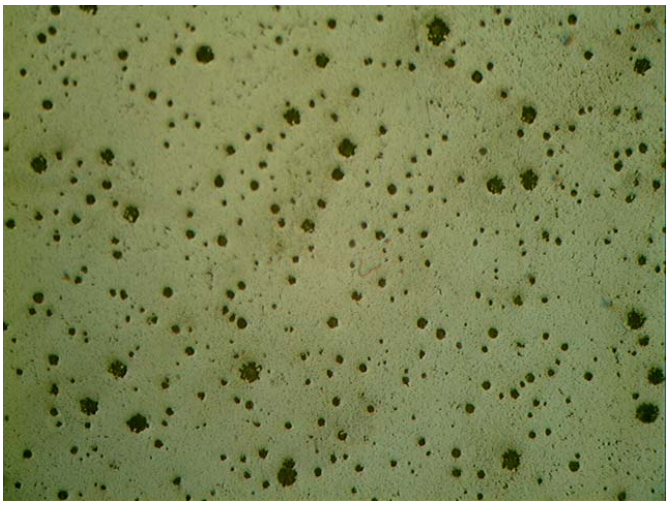

Figure 4.45 Optical Micrograph Showing Ductile Iron (2), 200 X.

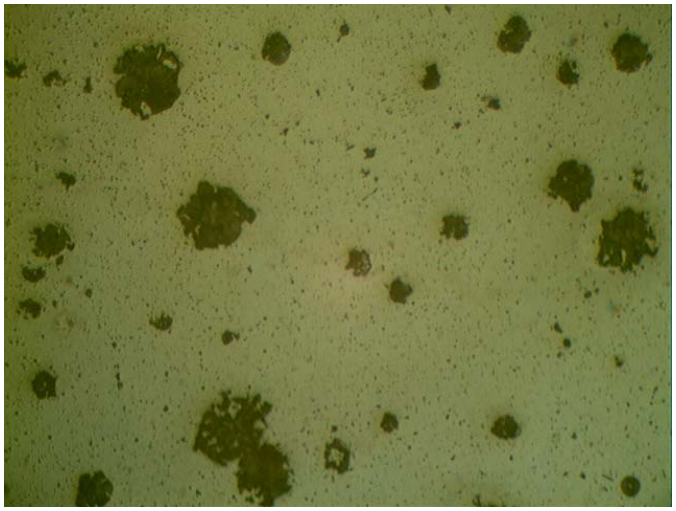

Figure 4.46 Optical Micrograph Showing Ductile Iron (2), 400 X.

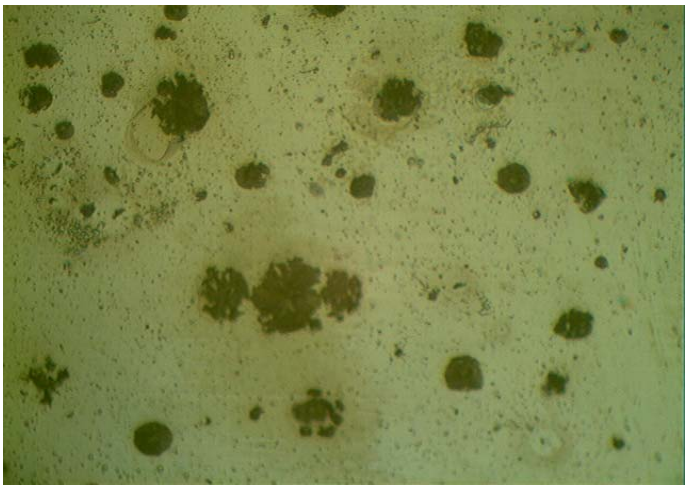

Figure 4.47 Optical Micrograph Showing Ductile Iron (2), Etched with 2 % Nital, 400 X.

As seen from the above microstructures, the shape of graphites are nodular and better than the results of the first ductile iron experiment. The main reason of this result is the whole process was completed before seven minutes, in other words the second experiment was done in a shorter time.

The cooling curve of the ductile iron gave us the solid fraction values by using Newtonian Thermal Analysis as discussed in the previous chapter.

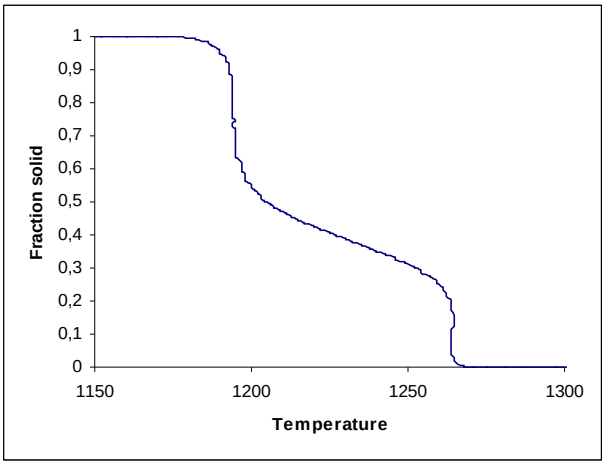

Figure 4.48 Solid Fractions of Ductile Iron by Temperature (°C).

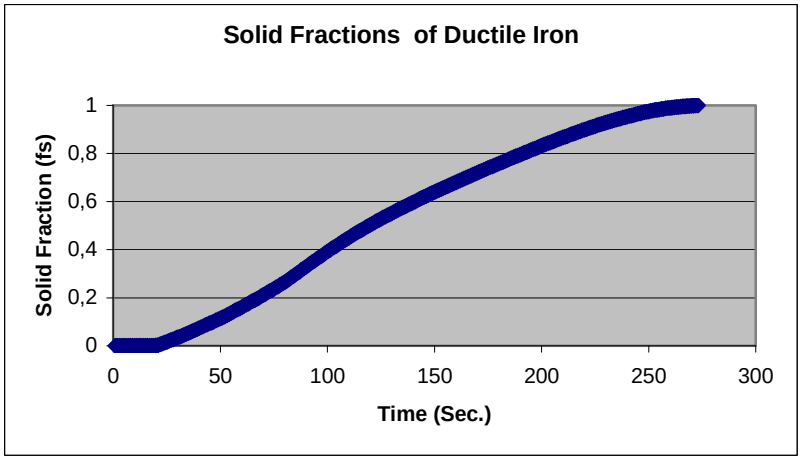

Figure 4.49 Solid Fractions of Grey Cast Iron by Time (Sec.).

By using the diagrams which are shown Figures 4.48 and 4.49, the solid fractions by temperature and by time can be controlled. During the bi-metal producing experiment these graphs became a useful tool.

4.3.3 Final Bi-Metal Experiment

After investigating the high chromium cast iron and ductile iron, final bi-metal casting experiment was done. The casting conditions, especially solid fraction value were decided according the results of first part of bi-metal experiments.

By using the solid fraction graphs of ductile iron, the necessary temperature and time for casting the second material, high chromium cast iron, was decided.

Finally, two alloys were prepared in two different induction furnaces at the same time. At first, 16 % Cr white cast iron was poured and waited until the solid fraction of it became approximately 30 %. Then, the nodular (ductile) cast iron was poured at 1400 °C.

Table 4.10 Chemical Composition of Final Bi-Metal Specimen.

Material	C %	Si %	P %	S %	Mg %
Ductile Iron	3.50	2.50	0.01	0.01	0.04
16 % Cr White Cast Iron	2.66	0.76	0.03	0.01	-

For metallographic investigation, the bi-metal specimen were prepared and photographs of microstructures were taken by using an optical microscope with digital camera, as shown in Figure 4.50.

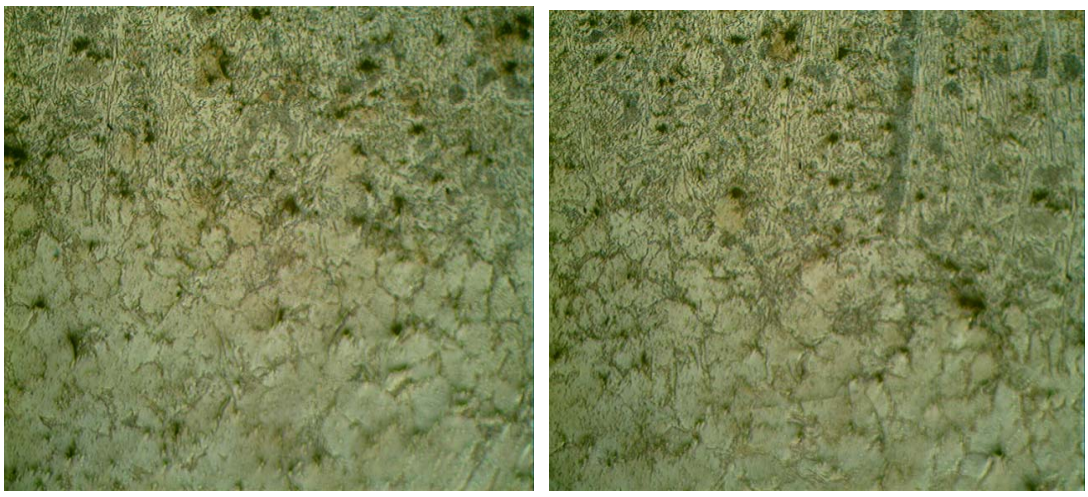

Figure 4.50 Optical Micrograph Showing Bi-Metal Specimen, 200 X.

4.4 A New Approach in White Cast Iron Production

High-chromium irons exhibit excellent abrasion resistance, and are therefore, used widely as a hard facing material in, e.g. the mining and mineral processing industry. In this case, a primary requirement is good abrasion and fracture resistance in cyclic

loading, high impact loading and corrosive environments. In addition, they are used in rolling/sliding contacts in applications such as work rolls for the hot rolling of metals, where the mechanisms of damage are abrasion of the matrix and rolling contact fatigue [30].

During solidification, chromium carbides are generated and these carbides promote the excellent wear performance of materials. But also, their low fracture toughness results in a brittle material. These carbides are often large (up to 0.5 mm long) and interconnected throughout the structure, and therefore, act as easy crack paths. [31]. Thus, much attention has been directed at the control of the shape, size, interconnectivity, volume fraction and distribution of the carbide phase by means of the addition of some modifier elements to the molten alloy [30-31].

In this part of the study, it was tried to obtain the same hardness value in an unalloyed white cast iron against high chromium white cast iron which is needed for resistance to abrasive wear, instead of using ferrochromium as an alloying material. Solidification pattern was changed.

The procedure is to promote the formation of cementite (Fe_3C) phase in the white cast iron by decreasing the eutectic temperature with cerium mischmetal addition and make a stable phase as iron carbide instead of chromium carbide observed high chromium irons.

In addition, the carbides are refined gradually and the morphology of primary carbides become more isotropic as cerium addition increases, but rather slowly when cerium addition exceeds 1.0 wt.% [32].

Table 4.11 Chemical Composition of Cerium Mischmetal.

Chemical Composition	Ce %	La %	Nd %	Pr %	Sm %	Other Heavies
Cerium Mischmetal	48 – 50	25 – 30	11 - 15	4 – 7	1 – 4	1 – 2

Table 4.12 Pysical Properties of Cerium Mischmetal.

Physical Properties	Melting Point	Specific Gravity	Atomic Number	Atomic Weight
Cerium Mischmetal	600 °C – 900 °C	6.67	57.71	140

4.4.1 Thermal Analysis

At first, unalloyed white cast iron and 0.2 % Ce white cast iron were prepared in induction furnace and by using thermal analysis quick cup, the cooling curves of them were obtained.

Table 4.13 Chemical Composition of Unalloyed White Cast Iron.

Unalloyed	C %	Si %	P %	S %
White Cast Iron	3.50	2.40	0.01	0.003

Table 4.14 Chemical Composition of 0.2 % Ce White Cast Iron.

Mischmetal Alloyed	C %	Si %	P %	S %
0.2 % Ce White Cast Iron	3.30	2.30	0.06	0.05

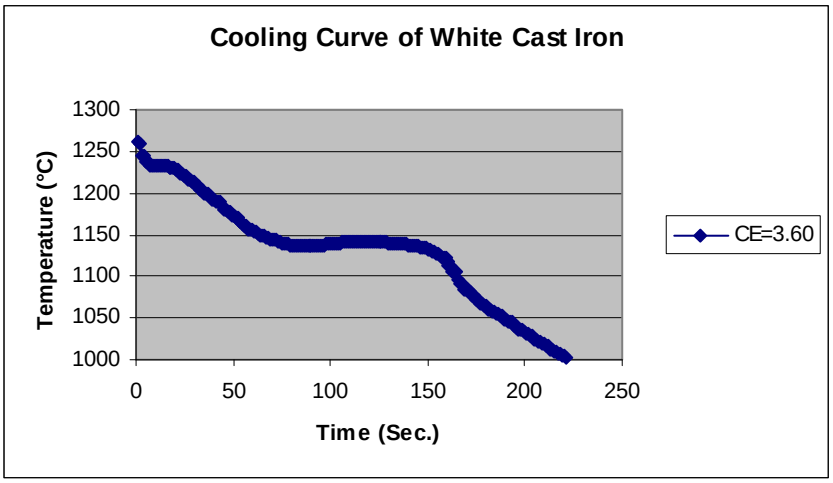

Figure 4.51 Cooling Curve of Unalloyed White Cast Iron.

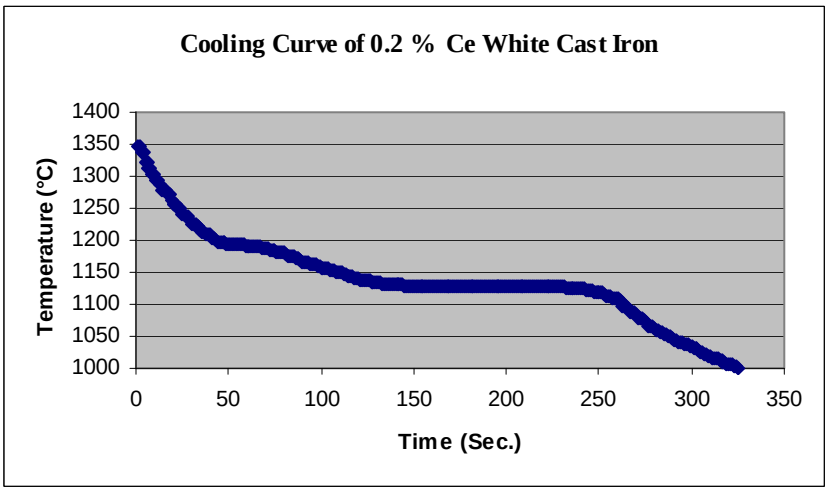

Figure 4.52 Cooling Curve of 0.2 % Ce White Cast Iron.

As shown in Figures 4.51 and 4.52, the eutectic temperature of unalloyed white cast iron is 1142 °C, whereas the eutectic temperature of 0.2 % Ce white cast iron is 1128 °C.

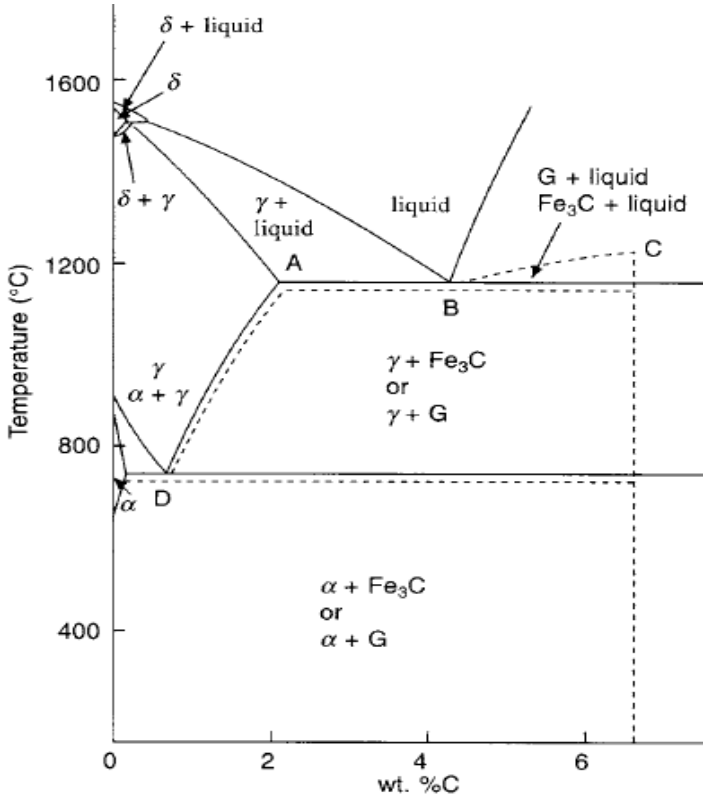

Figure 4.53 Iron-Cementite Phase Diagram.

As shown in Figure 4.53, the stable phase under eutectic point is cementite (Fe_3C) and by decreasing the eutectic temperature, the ratio of cementite in the matrix will increase.

4.4.2 Hardness Test

The main aim was to obtain the same hardness value with high chromium white cast iron. Thus, ferrochromium would not be used as an alloying material. Only, small percent of cerium mischmetal would be used. Obtaining the same hardness value with 12 % Cr white cast iron was succeeded with using only 0.2 % Ce addition.

At first, unalloyed white cast iron and 0.2 % Ce white cast iron were prepared in induction furnace and hardness test specimens were poured.

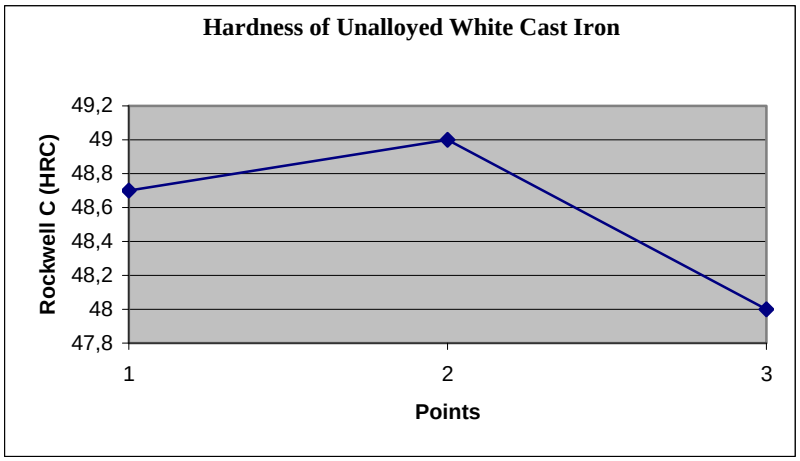

Figure 4.54 Hardness Test Result of Unalloyed White Cast Iron.

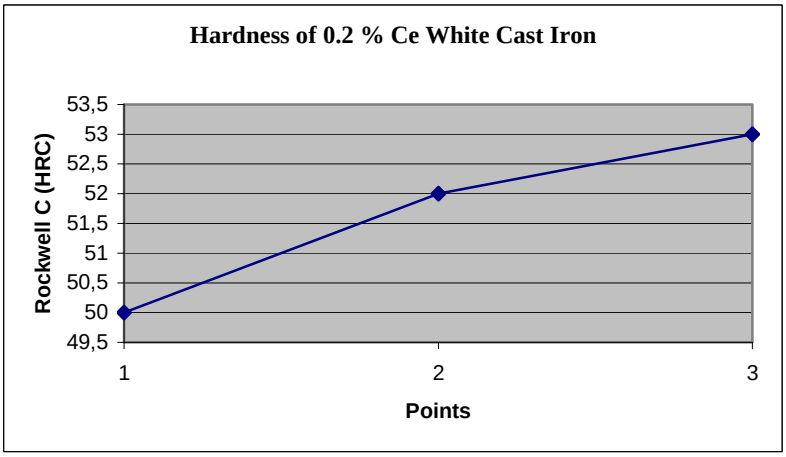

Figure 4.55 Hardness Test Result of 0.2 % Ce White Cast Iron.

The hardness test results of two material, Figures 4.54 and 4.55, showed that the average hardness value of unalloyed white cast iron is 49 HRC and the average

hardness value of 0.2 % Ce white cast iron is 53 HRC. These values also correspond to 470 BHN and 512 BHN.

From the ASM A-532 Standard, the hardness value of 0.2 % Ce white cast iron approximately correspond the hardness value of 12 % Cr white cast iron. Hence, 12 % Cr white cast iron was prepared in induction furnace and hardness test specimen was poured.

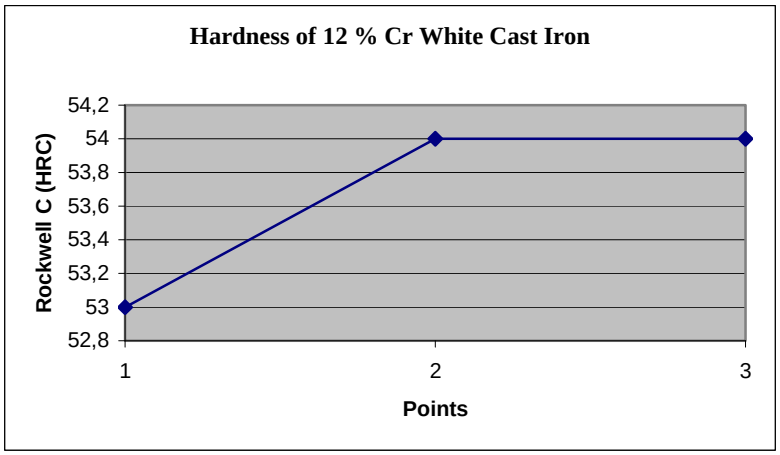

Figure 4.56 Hardness Test Result of 12 % Cr White Cast Iron.

As shown in Figure 4.56, the hardness value of 12 % Cr white cast iron is 54 HRC. It also corresponds to 540 BHN.

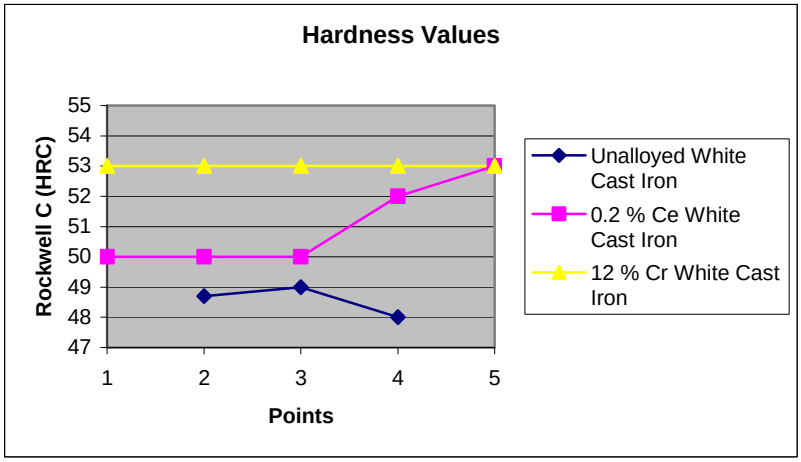

Figure 4.57 Hardness Test Results of Three Different White Cast Irons.

As it can be seen from Figure 4.57, the hardness values of unalloyed, 0.2 % Ce and 12 % Cr white cast irons are approximately the same.

4.4.3 Metallographic Investigation

For metallographic investigation and comparison of the microstructures at different magnifications, the specimens of unalloyed white cast iron, 0.2 % Ce white cast iron, 12 % Cr white cast iron, and 16 % Cr, 0.2 % Ce white cast iron specimens were prepared and photographs of microstructures were taken by using an optical microscope with digital camera.

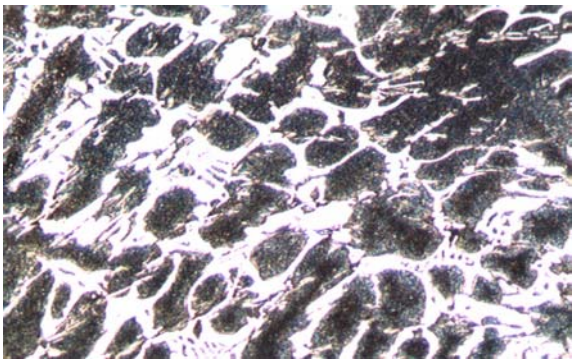

Figure 4.58 Optical Micrograph Showing Unalloyed White Cast Iron, 100 X.

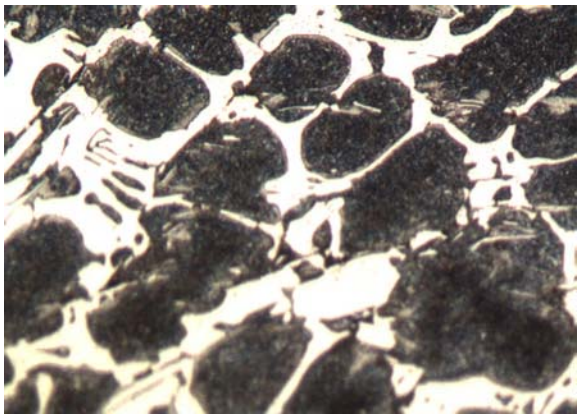

Figure 4.59 Optical Micrograph Showing Unalloyed White Cast Iron, 200 X.

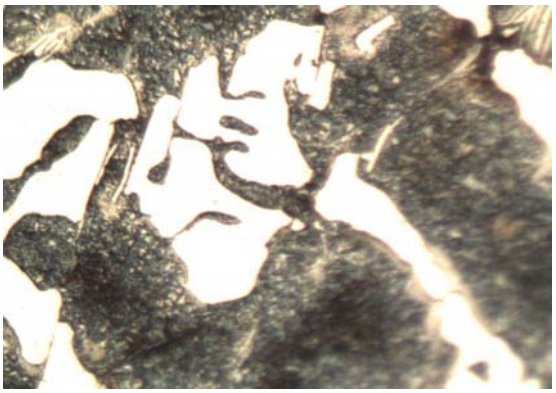

Figure 4.60 Optical Micrograph Showing Unalloyed White Cast Iron, 500 X.

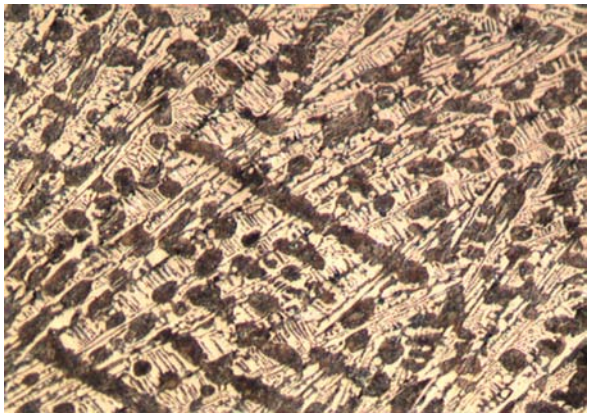

Figure 4.61 Optical Micrograph Showing 0.2 % Ce White Cast Iron, 100 X.

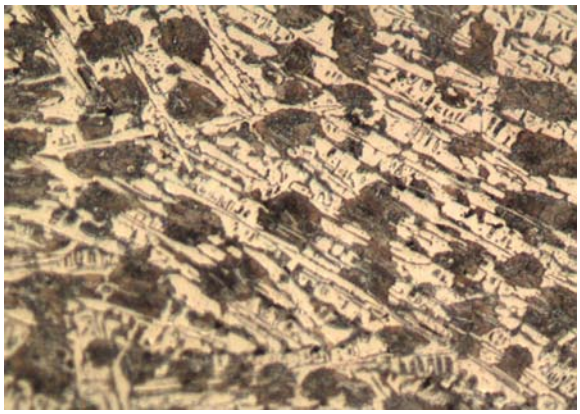

Figure 4.62 Optical Micrograph Showing 0.2 % Ce White Cast Iron, 200 X.

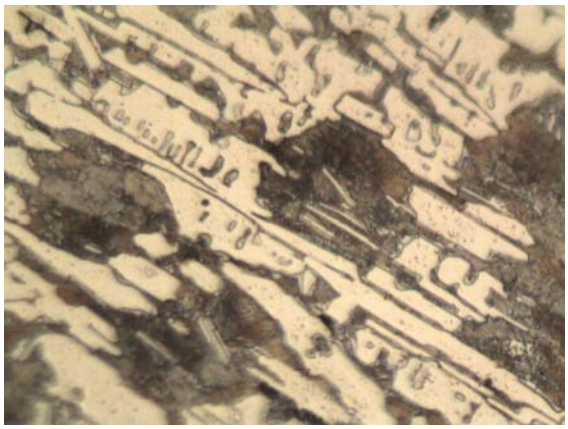

Figure 4.63 Optical Micrograph Showing 0.2 % Ce White Cast Iron, 500 X.

Figures 4.61, 4.62 and 4.63 show the typical microstructures obtained by cerium treatments.

These micrograps were taken at the same magnification and it is seen that the size of transformed austenite phases is bigger in unalloyed white cast iron. As it is known, the smaller grains improve the mechanical properties of the material.

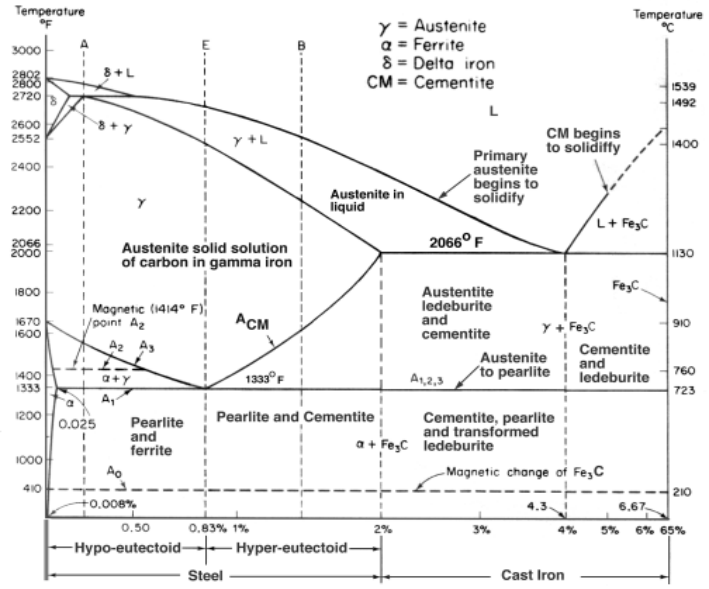

Figure 4.64 Iron – Carbon Phase Diagram.

As shown in Table 4.13, the chemical composition of unalloyed white cast iron specimen gave the carbon equivalent value 4.30. It means that, it is eutectic point. As can be seen from Figure 4.64, under eutectic point, austenite, ledeburite and secondary cementite are the metastable phases. By using cerium mischmetal addition, the eutectic temperature decreased and also the size of the transformed austenite and ledeburite decreased.

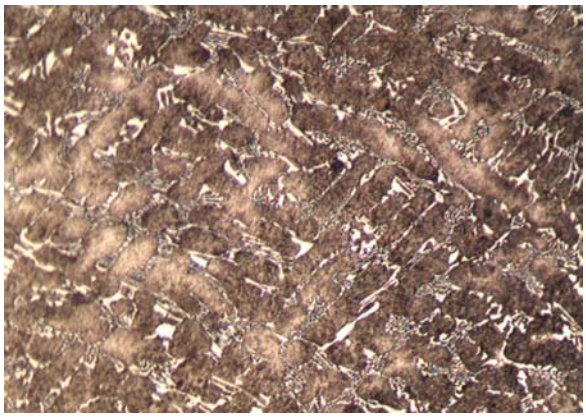

Figure 4.65 Optical Micrograph Showing 12 % Cr White Cast Iron, 100 X.

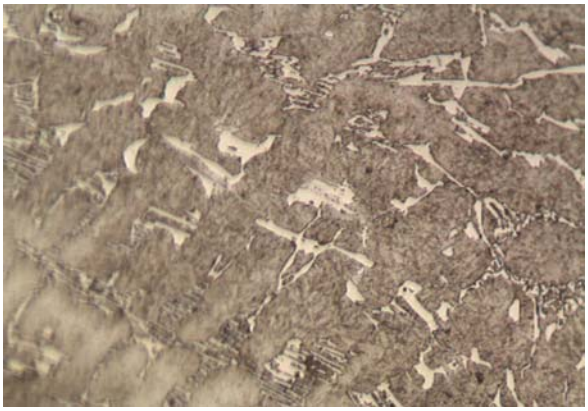

Figure 4.66 Optical Micrograph Showing 12 % Cr White Cast Iron, 200 X.

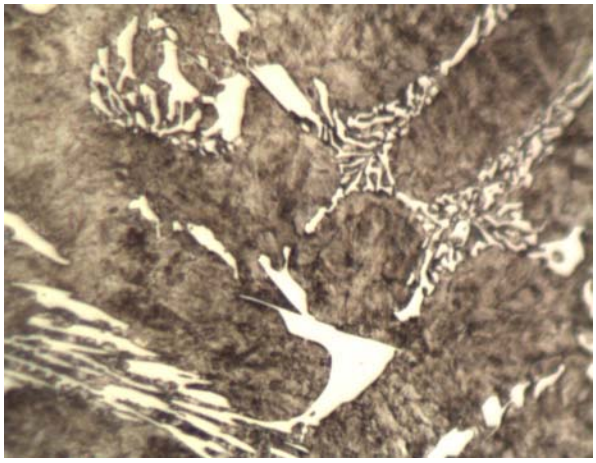

Figure 4.67 Optical Micrograph Showing 12 % Cr White Cast Iron, 500 X.

Figures 4.65, 4.66 and 4.67 show the micrographs of 12 % Cr white cast iron which has approximately the same hardness value with 0.2 % Ce white cast iron. The main difference is, the high chromium cast irons provide the hardness value with the chromium-rich carbide formation whereas in white cast irons, there are cementite (iron carbide) phases that provide the high hardness.

4.4.4 Carbide Extraction Method

There are different types of carbides. Identification of these carbides is very important to evaluate mechanical properties of the materials. Carbide extraction method aims at obtaining the hard carbides from the main matrix. Than, these carbides will be used as XRD analysis specimen and it will give the best result to learn types of them [33].

Carbide extraction from the specimens was performed in an electrolytic cell which is connected to a direct current source and containing stainless steel sheets as the cathode, as shown in 4.68.

12 % Cr white cast iron specimen, before being put into the cell as the anode, was washed in alcohol and weighted. Extraction was carried out at a current density 0.01-0.04 A / cm2 in an electrolyte of 10 % HCl-distilled water. Extraction time was 24 hours.

Figure 4.68 Experimental Set-Up for Carbide Extraction

At the end of the extraction process, carbide residues were collected in a filter paper and washed with fresh electrolyte and dried.

4.4.5 X-Ray Analysis

After carbide extraction of 12 % Cr white cast iron, the carbide specimens from extraction were analysied by X-Ray. According to X-Ray results, carbide type was found as Cr_7C_3 , as shown in Figure 4.69.

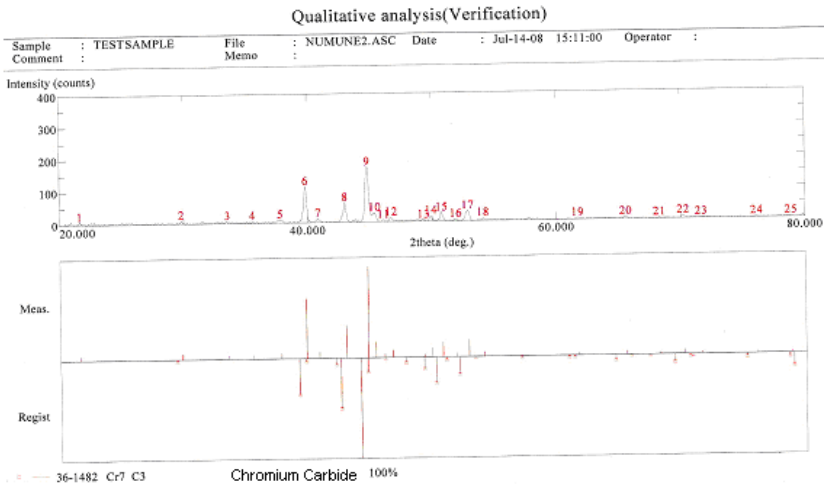

Figure 4.69 XRD pattern of 12 % Cr White Cast Iron, Qualitative analysis

4.4.6 SEM Investigation

By using scanning electron microscope, the detailed and close views of microstructures were evaluated and photographs of them were taken. In addition, energy dispersive X-ray analysis (EDX) was made for two different phases.

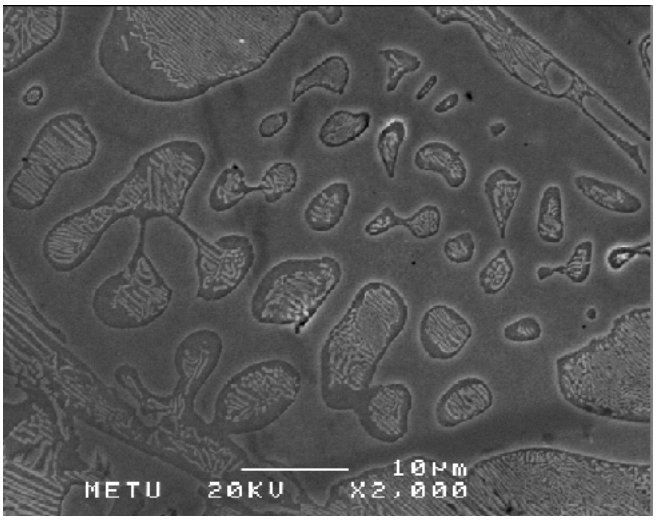

Figure 4.70 SEM Micrograph of 0.2 % Ce White Cast Iron, 2000 X.

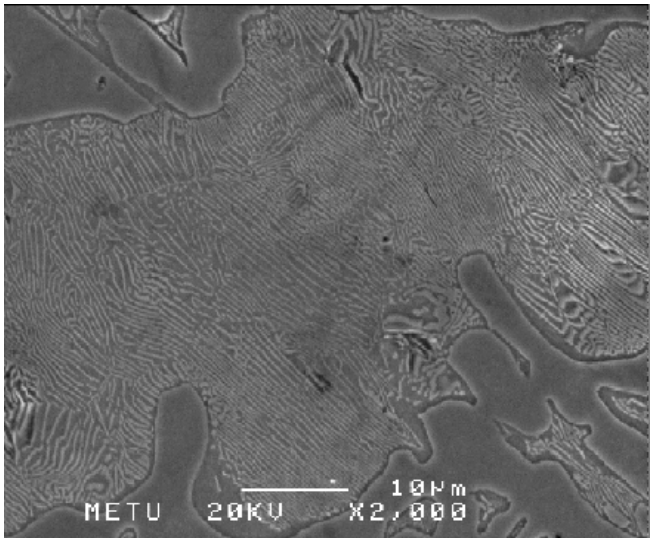

Figure 4.71 SEM Micrograph of 0.2 % Ce White Cast Iron, 2000 X.

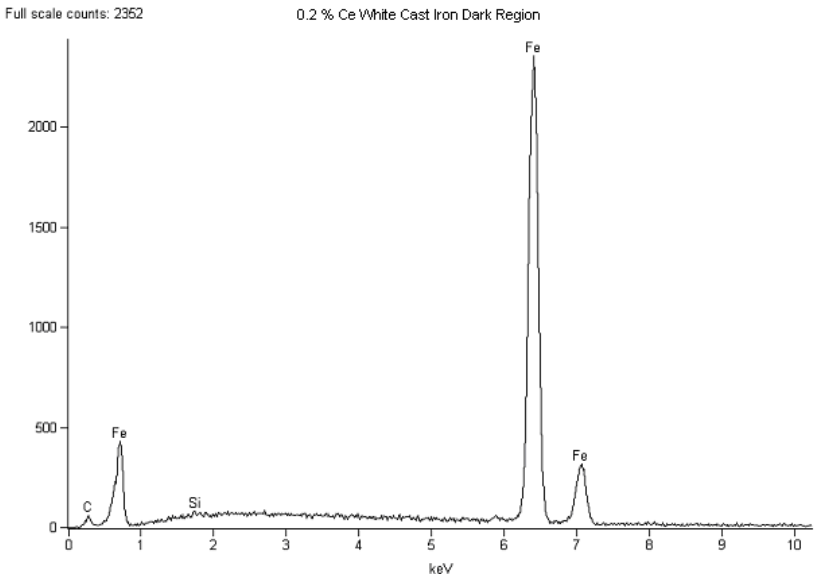

Table 4.15 EDX Analysis of 0.2 % Ce White Cast Iron, Dark Region.

Element	*Weight Conc %*	*Atom Conc %*
Si	0.25	0.50
Fe	99.75	99.50

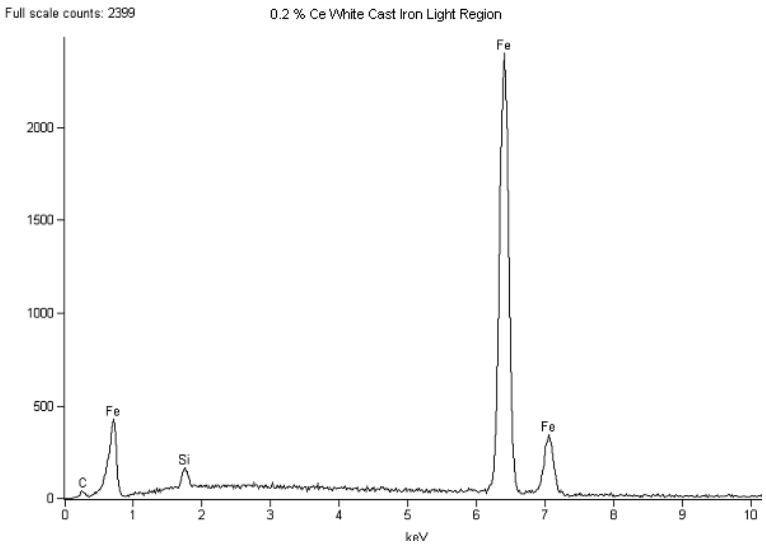

Table 4.16 EDX Analysis of 0.2 % Ce White Cast Iron, Light Region.

Element	*Weight Conc %*	*Atom Conc %*
Si	1.67	3.26
Fe	98.33	96.74

4.4.7 Mechanical Tests

For evaluation of the mechanical properties of the specimens, hardness test and tensile test were done.

4.4.7.1 Hardness Test

For this part of the study, the most important mechanical test is hardness measurement. Because the main aim was to obtain same hardness value without using ferrochromium alloy.

Table 4.17 Hardness Test Results.

Hardness Test	Unalloyed White Cast Iron	12 % Cr White Cast Iron	0.2 % Ce White Cast Iron
As-Cast	470 BHN	550 BHN	520 BHN
After Stress Relieving	400 BHN	481 BHN	450 BHN

4.4.7.2 Tensile Test

The tensile test specimens were prepared and their tests were done using 5000 kg-force tensile test machine.

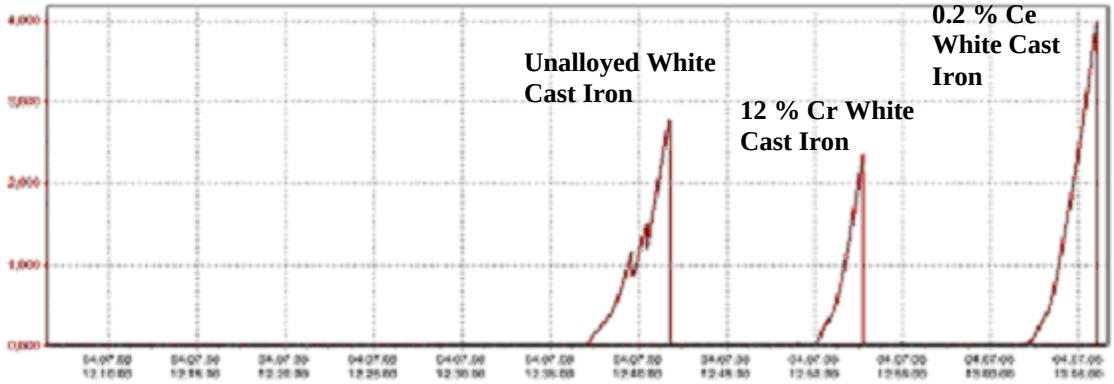

Figure 4.72 Tensile Test Results.

Table 4.18 Tensile Strength Results.

Material	Tensile Strength, MPa
Unalloyed white cast iron	280
12 % Cr white cast iron	250
0.2 % Ce white cast iron	400

Figure 4.72 and Table 4.18 show the tensile test results of, unalloyed white cast iron, 12 % Cr white cast iron and 0.2 % Ce white cast iron. As can be seen from the results, 0.2 % Ce white cast iron has the highest tensile strength. The carbides are refined gradually and the morphology of primary carbides become more isotropic with cerium addition [32]. Shape of carbides become more isotropic with cerium addition and so fracture toughness of carbides increases. Also, this affected the tensile strength of the specimen.

4.4.7.3 Impact Test

For the same three material, impact test specimens were also prepared and charpy impact test was made. There is not big difference between them. Average toughness value is 2 joule. As also seen from tensile test, there is no yield point in these materials and their toughness values are very low.

CHAPTER 5

CONCLUSION

In this study, the failure analysis of Hadfield steel impact bar which is used in coal grinders and crushers had been made. The results of failure analysis showed that, there is not enough impact for Hadfield steel communition machine parts to realize phase transformation from austenite to martensite. Thus, the hardness value which is necessary for resistance to abrasion is not obtained in Hadfield steels.

Abrasive conditions result in the progressive removal of material and due to various phase transformations from austenite to martensite introduces surface volume changes and causes the generation of cracks and further lead the failure of the component.

The objective of the present study was to find a possible solution for the wear problem which is seen in Hadfield steel communition machine parts. The possible solution is bi-metal which have two main parts. The first part is wear resistant part and high chromium white cast iron was choosen for its high resistance to abrasion. The second part of bi-metals is tough part and ductile iron was choosen because of its high toughness property.

The basic principle for producing bi-metals was to obtain the best solid fractions to make the interface behave as a third phase between two different materials. For this reason, different bi-metal producing experiments was done under different experimental conditions. Thermal analysis of the materials and mechanical tests of the bi-metal specimens were performed and results were evaluated.

The results of the experiments showed that, for white cast iron and gray iron duplex structure recommended pouring temperature of white cast iron is 1150 °C -1180 °C.

The gray cast iron is poured at 1400 °C on to this white cast iron. In this temperature range, solid fraction values were calculated as 40 % and 30 % for white cast iron.

For high toughness the spheroidal graphite cast iron was choosen and produced instead of low carbon steel which is being used in todays' technology.

The second objective of this study was to find an alternative way to obtain same hardness value in white cast iron, instead of using ferrochromium. The aim was, decreasing the eutectic temperature of the white cast iron to increase the ratio of cementite phase in the matrix.

Cerium mischmetal was used as an alloying material in white cast irons. 0.2 % Ce white cast iron was produced and it was seen that the eutectic temperature decreased from 1142 °C to 1128 °C. In addition, the hardness value increased from 470 BHN to 520 BHN.

The hardness value of 0.2 % Ce white cast iron is approximately the same with 12 % Cr white cast iron. To get 520 HB hardness value ; 50 g cerium mischmetal was used instead of 3300 g FeCr in 10,000 g raw material. 3300 g FeCr is 26.4 Euro, whereas 50 g Cerium Mischmetal is 1 Euro.

Tensile test and impact test specimens of unalloyed white cast iron, 0.2 % Ce white cast iron and 12 % Cr white cast iron were prepared and their mechanical tests were done. The results showed that, tensile strenghts of unalloyed and 12 % Cr white cast irons are approximately the same whereas 0.2 % Ce white cast iron has higher tensile strenght. All of them have low toughness values.

In addition, the carbides are refined gradually and the morphology of primary carbides become more isotropic with cerium addition [32]. Shape of carbides become more isotropic with cerium addition and so fracture toughness of carbides increases.

Future work suggestions :

1) New experiments can be done in the 25 % - 40 % solid fraction range. Mechanical tests can be developed for interface control.
2) Mold design for bi-metal production can be modified and interface control during experiment can be made more efficiently.
3) Bi-metal technology can be applied for different applications and different materials can be used for different aims.

REFERENCES

[1] World Coal Institute, " The Coal Resource: A Comprehensive Overview of Coal", http://www.worldcoal.org, 01/01/2007.

[2] Gießereitechnologie GmbH, Magdeburg Germany, "Experience with the Use of Composite Cast Hammers in the Cement Industry", ZKG International-No.2/2000 Vol. 53

[3] E. J. Pryor , "Mineral Processing", 3rd edition, Applied Science Publishers Limited, University of London, (1965)

[4] L. Weiss, Editor in Chief, "Mineral Processing Handbook", Society of Mining Engineering, New York, (1985).

[5] W. Leonard and R. Mitchell, Editors , "Coal Preparation", The American Institute of Mining, Metallurgical and Petroleum Engineers, Inc., New York, (1968).

[6] M. B. Peterson and W. O. Winer, "Wear Control Handbook", The American Society of Mechanical Engineers, New York, (1980).

[7] S. Alyaz, "Effects of Heat Treatment and Chemical Composition on Microstructure and Mechanical Properties of Hadfield Steels", METU M.S. Thesis, December 2003

[8] N. Petrov, G. Gavriljuk, H. Berns, F. Schmalt, "Surface Structure of Stainless and Hadfield Steel after Impact Wear", Wear Vol.260 (2006) pp.687-691

[9] E. W. Colbeck, "Manganese Steel", Hadfields Limited, London, (1956)

[10] E. Bayraktar, F. A. Khalid, C. Levailant, “Deformation and Fracture Behaviour of High Manganese Austenitic Steel”, Journal of Materials Processing Technology, Vol.147 (2004), pp.145-154

[11] R. Zavadil, S. Kuyucak, “Microstructure vs. Impact Toughness Relationship in Hadfield’s Austenitic Manganese Steel”, Microscopy Society of America,(2002)

[12] H. T. Angus, “Cast Iron: Physical and Engineering Properties”, 2nd edition British Cast Iron Research Association, (1976).

[13] M. A. Gonzalez and H. K. D. H. Bhadeshia, “Cast Irons”, Department of Materials Science and Metallurgy, Universty of Cambridge, (2000)

[14] CP. Tabret,IR. Sare ,“Fracture Toughness of High-chromium White Irons; Influence of Cast Structure”, J. Mater Sci. (2000)

[15] D. On, JA. Hawk, G. Laird, “Solidification Structure and Abrasion Resistance of High Chromium White Irons”, Metall Mater Trans. A Phys Metall Mater Sci. June 1997; 28 A.

[16] A. Adler and N. Dogan, “Erosive Wear and Impact Damage of High-Chromium White Cast Irons”, US Department of Energy, Albany Research Center, (2000).

[17] J. Asensio, J. A. Pero-Sanz and J. I. Verdeja, “Microstructure Selection Criteria for Cast Irons With More Than 10 wt.% Chromium for Wear Applications”, Department of Materials Science and Metallurgical Engineering, Spain, (2002)

[18] D. Mullins, “Ductile Iron Data for Design Engineers”, Rio Tinto Iron and Titanium Inc., Canada (1990)

[19] Foseco Ferrous Foundrymens’ Handbook, 11nd edition, (1994)

[20] Dr. Jae-Young JUNG, “Bimetallic Casting Wear-resistant Materials”, Metallic Materials and Coating Process Research Team, Pohang, Korea Research Institue of Industrial Science and Technology, (2000)

[21] E.I. Marukovich, A. M. Branovitsky, Y. S. Na, J. H. Lee, K. Y. Choi, “Study on the Possibility of Continuous-casting of Bimetallic Components in Condition of Direct Connection of Metals in a Liquid State”, Materials and Design Vol.27 (2006) pp.1016-1026

[22] Dr. Ing Hans Wahl GmbH, Vautid-Verschleiss-Technik,“ Vautid-Bimetal Casting”, Stuttgart, (2000)

[23] R. D. Shull and A. Joshi, “Thermal Analysis in Metallurgy”, TMS Minerals, Metals, Materials, (1990).

[24] R. F. Speyer, “Thermal Analysis of Materials”, School of Materials Science and Engineering, Georgia Institute of Technology, Atlanta, Georgia, (1994).

[25] M. R. Chavez, A. Amaro, C. Flores, A. Juarez, C. Gonzalez-Rivera, “Newton Thermal Analysis of Gray and Nodular Eutectic Cast Iron”, Materials Science Forum Vol. 509 (2006), pp. 153-158.

[26] U. Hemmann, “Reduction of Wear and Abrasion, Long-Life Cast Hammers for the Cement Industry”, HARDTOP, Gießereitechnologie GmbH, Magdeburg Germany, 2000.

[27] T. Teeri, V. T. Kuokkala, P. Siitonen, P. Reponen and J. Liimatainen, “Impact Wear in Mineral Crushing”, Proc. Estonian Acad. Sci. Eng. (2006), Vol.12, pp.408-418.

[28] K. Venkateswarlu, S. G. Chowdhury, L. C. Pathak, A. K. Ray, “Microstructural Examination of Service Exposed Coal Mill Liner Material”, Materials Characterization, Vol. 58 (2007), pp.1029-1032.

[29] R. G. Wellman, C. Allen, “The Effects of Angle of Impact and Material Properties on the Erosion Rates of Ceramics”, Wear (1995); 186-187 : 117-22.

[30] A. B. Jacuinde, W. M. Rainforth, “The Wear Behaviour of High-Chromium White Cast Iron as a Function of Silicon and Mischmetal Content”, Wear, Vol.250 (2001), pp. 449-461

[31] P. A. Morton, R. B. Gundlach, J. Dodd, AFS Trans. 93 (1985) 879.

[32] Y. Qu, J. Xing, X. Zhi, J. Peng, H. Fu, “Effect of Cerium on the As-Cast Microstructure of a Hypereutectic High Chromium Cast Iron”, Materials Letters, (2008)

[33] B. Ogel, “ The Effect of Double Austenitization on Microstructure And Fracture Toughness of AISI M2 High Speed Steel”, Ph. D. Thesis, METU, (1990).